STAND OFF BOMB DETECTION USING NEUTRON INTERROGATION

by

JUSTIN LOWREY

B.S., Kansas State University, 2006

A THESIS

submitted in partial fulfillment of the requirements for the degree

MASTER OF SCIENCE

Department of Mechanical and Nuclear Engineering
College of Engineering

KANSAS STATE UNIVERSITY
Manhattan, Kansas

2008

Approved by:

Major Professor
Dr. William L. Dunn

Abstract

One of the most pressing threats facing the United States is the increasingly effective use of improvised explosive devices or IEDs. Many commonly used techniques to detect explosives involve imaging. The primary drawback of imaging is that it requires interpretation of one or more images from each target. Human interpretation requires extensive training and is subject to the chance of false-negatives due to human fatigue.

To counter the threat posed by IEDs, the signature-based radiation scanning (SBRS) technology has been developed. The goal of this project is to create an automated system, with minimal operator assistance, that is capable of detecting at least a gallon-sized explosive sample from at least one meter away. It is hoped that this can be accomplished quickly, in less than 30 seconds, with high sensitivity and specificity. The SBRS technique is based on the fact that many classes of materials have similar stoichiometries. For example, many common explosives have characteristic concentrations of hydrogen, carbon, nitrogen and oxygen. As neutrons interact with a material, unique gamma rays are created based on the composition of the material. Specifically, in this work, the gamma rays from inelastically scattered neutrons and from thermal neutron capture are investigated. Two neutron detectors are also used, whose responses depend on neutron thermalization in and around the target. Response templates are created based on gamma-ray and neutron responses that are collected from targets that contain explosives,. These templates are developed under different conditions for many different explosive materials to create a library of templates. The collection of responses from an unknown target is compared to a subset of the library of templates using a figure of merit to distinguish benign from explosive targets.

Preliminary experiments were performed at Kansas State University. A high-purity germanium detector (HPGe) was used to detect the gamma rays. Two neutron detectors, one covered with cadmium, were used to detect back-streaming neutrons. A ^{252}Cf radioisotope source as well as a Triga Mk III reactor were used as neutron sources.

Copyright

Table of Contents

List of Figures

List of Tables

Acknowledgements

I would like to thank Dr. Dunn for allowing me to work on this project and M2 Technology for their funding and support. I would also like to thank Kennard Calendar for his work on the weighting factors and all of the undergraduates who worked on this project for their hard work.

Dedication

This work is dedicated to my family, whose support has gotten me to where I am.

CHAPTER 1 - Introduction

1.1 The IED Problem

An IED is defined as "a device placed or fabricated in an improvised manner incorporating destructive, lethal, noxious, pyrotechnic, or incendiary chemicals and designed to destroy, incapacitate, harass, or distract. It may incorporate military stores, but is normally devised from nonmilitary components" [1]. As of June 30, 2008, 1710 of 4113 recorded American casualties in Iraq, over 40%, were due to IEDs [1]. It is obvious that these devices present a clear and present danger to soldiers and civilians around the world. A solution to identify and remove these dangerous devices is imperative.

IEDs are not a new technology. They have been used in conflicts throughout the world. They have notable places in history including derailing trains in World War II and being used as tools of assassinations. The materials used in explosive devices are usually widely available in war-torn regions. This is often the case due to the proliferation of weapons that occurs during war and from unexploded ordnance that can be found during conflict. These devices are perfect for guerrilla tactics as they are inexpensive and simple and can be used with much less risk than a fighter encounters in open combat. Their basic construction includes two parts: an explosive charge and a detonation system.

The explosive charge can be some home-made substance or a high yield military explosive. The most prolific use of IEDs in the world is happening in the current Iraq conflict, which is an area that has known conflict for decades. Many of these IEDs use old military artillery shells very effectively. These devices are often created for a specific purpose. IEDs can be designed to be anti-personnel or to take out armored targets. Surrounding an explosive with shrapnel, such as ball bearings or nails, has proven to be a very simple and effective anti personal device. IEDs can take out armored targets with explosively formed penetrators. This is usually done by a shaped charge that focuses the pressure from an explosive to compress and accelerate a metal slug which then cuts through armor.

There are numerous different detonation systems. An IED can be triggered by an operator using a radio or infrared controlled remote. IEDs can also be designed to detonate automatically by magnetic trigger, pressure sensors or a timer. The electronics for these

detonation systems can be sophisticated, but more often than not, are scavenged from common electronics. Cell phones, remote control toys, garage door openers, kitchen timers and alarm clocks all can be converted, with minimal electronic knowledge, to detonation systems.

IEDs are used in a variety of ways. They can be placed in high traffic areas with the goal of hitting a target as it passes or they can be delivered to a target by a vehicle. Devices left in hiding are often buried under the road with the goal of detonating as a vehicle passes. These are particularly effective as the vulnerable undersides of most vehicles house the fuel tank which can trigger secondary explosions and create additional shrapnel from the vehicle itself. The military has designated vehicle based IEDs as VBIED explosive devices. VBIEDs often carry several hundred pounds of explosives and can cause massive amounts of destruction and loss of life.

The threat from IEDs became apparent not long into the second Iraq conflict. As the number of deaths and injuries from these devices increased, the United States Army put together a special task force in the fall of 2004 to find solutions to the IED problem. This task force became a joint operation among the military branches led by the Army in July of 2004 [5]. The Joint Improvised Explosive Device Defeat Task Force, or JIEDD, has been given the job of coordinating all Department of Defense efforts to reduce the threat from IEDs. The fact that 1.23 billion dollars was allocated to JIEDD for the 2004 billing cycle shows how seriously the military views this threat.

1.2 The Goal

The goal of this research project was to develop neutron-based technology that can be used to detect IEDs that contain nitrogen-rich explosives. The detection system should be effective, mobile, rugged and reliable in detecting a wide variety of IEDs at a distance exceeding a meter. Fulfillment of this goal is a daunting task. The material this thesis covers concerns the proof of concept and prototyping phase of a detection system that uses the signature based radiation scanning (SBRS) method. The initial project goals were divided as follows:

- Forward Looking – All equipment for the system would need to be operated from one side of the target
- High Sensitivity and Good Specificity – A system is needed that has a low false-negative rate; that is, the system would rarely declare a target safe when it was in

fact dangerous. A system with low false-positives is also desired; that is, the system would rarely declare a target dangerous when it is not.

- Stand-off Distances – The system needs to be able to detect explosives from some distance. Ideally, a detection system should operate from a range of several meters. For the initial experiments, the goal was to operate from more than one meter.
- Small Amounts – There is also the need to detect relatively small amounts of explosive; the initial goal is to be able to detect amounts as small as a gallon (approximately 8 pounds).
- Automated Analysis – Finally, there is a need to have a system that requires minimal user interface. The computer will collect the data, analyze it, and finally display to the operator a safe or potentially dangerous indication.

1.3 Outline of Thesis

Existing IED detection methods are reviewed in Chapter 2. These methods are divided into the sub-groups of protection, prevention and detection. In the protection section, the benefits and drawbacks of armor are considered. A variety of technologies can be used to prevent destruction from IEDs, including technologies to help avoid IEDs and others to prevent their detonation. An overview of some of these methods is covered in the prevention section. Finally, both bulk and trace detection methods are considered.

The methodology behind the neutron interrogation based explosive detection approach investigated is considered in Chapter 3. The three key neutron interactions of prompt neutron capture, inelastic neutron scatter, and neutron thermalization are reviewed. The special considerations needed for high-energy gamma-ray detection are also considered.

An overview of some experiments conducted for this project is given in Chapter 4. Two separate neutron sources were used and the benefits and drawbacks of each are considered. The equipment and the experiment arrangements are described.

The analysis process and the experimental results are described in Chapter 5. The specifics of a template matching procedure are explained and the signatures used in the analysis process are identified. A figure-of-merit and its standard deviation are described and a filter

function is used to distinguish inert from explosive targets. Results from the two reactor based experiments are given.

A summary of the explosive detection method is given in Chapter 6. The results are reviewed and the benefits and challenges of the method are considered. Some recommendations are given about how to potentially improve the method. The planned next steps in the project are also discussed.

CHAPTER 2 - Previous IED Detection Efforts

Attempts to prevent loss of life from IEDs can be categorized into three groups; detection, prevention, and protection. Detection can categorize a wide variety of systems and methods, all with the goal of identifying and or locating an explosive device. If IEDs can not be located, the next best thing is to prevent their detonation. This can be done by interfering with the device's circuitry or detonator, or by identifying suspicious areas and avoiding them. Finally, if an IED can not be detected or avoided, the last line of defense is protection. New and more advanced armor can protect humans and save lives. An important distinction in IED detection technology is remote detection versus standoff detection. Remote detection means the operator could be at a distance, but the equipment would need to be close to the target to operate. Standoff detection is defined as having both the equipment and the operator at safe distances. Logically, standoff detection is preferred due to the dual protection offered. Moreover, remote detection systems, as opposed to standoff detection systems, will be either stationary or robotically-controlled, which can be problematic in a rugged field environment.

2.1 Protection

Initially, the U.S. Military responded to the increasing threat from IEDs by armoring vehicles. By June 2005, there were between 9,000 and 12,000 high mobility multipurpose wheeled vehicles (HMMWV) in Iraq that were armored [2]. This was an effective first step, and initially the armor could shield against the relatively simple IEDs being used in the early days of the conflict. However, it did not take long before IED builders adapted and created more effective weapons that were capable of taking out the reinforced vehicles. The early IEDs were referred to as "double-bangers" and were usually made from artillery rounds. The more advanced devices were referred to as "five-bangers" and could destroy HMMWVs [2]. An embedded journalist, Michael Yon, was quoted as saying, "The enemy has destroyed our most powerful armored tanks with underground bombs that leave craters in the roads large enough to make swimming pools. No amount of armor can completely protect us. Armor is extremely important, but given time, the enemy will defeat it."[2].

2.2 Prevention

There are many ways to prevent loss of life from IEDs. This can be achieved either by identifying potentially dangerous areas or by preventing the detonation of the explosive device. The following is an overview of some of the technologies being used and developed to prevent injury and deaths from IEDs.

Electronic Jammers – Electronic Jammers were the first IED countermeasures widely used in Iraq. These devices work by using low-power radio frequency energy to jam cell phones, satellite phones, cordless phones and other types of remote detonators [3]. These devices are versatile and can be vehicle-mounted or handheld [2]. In response to the increasing frequency and lethality of IEDs, Defense Secretary Donald Rumsfeld directed the Army to buy 10,000 Warlock Blue devices, which were the first generation of jammers, in May 2005 [2]. These devices are only effective against IEDs that use radio wave remote detonators. This technology can be completely circumvented by using infrared detonators, like garage door openers, or pressure detonators. Another problem has been reports of jammers interfering with the radios used by soldiers [3]. This results in soldiers having to shut off their jammers to use the radio thereby creating windows of vulnerability. In addition, a new problem has become apparent with the increased use of unmanned aerial vehicles or UAVs. Specifically, the UAVs can lose their radio frequency control links due to interference from these jammers when they are away from their control base [3]. In short, electronic jammer devices were very useful in the early battle against IEDs, being cheap and reliable against radio detonated bombs, but they are completely ineffective against bombs that do not use radio detonators, a fact that has become widely known and has made this technology less effective.

Imagery Analysis [2] - Another method to prevent loss of life from IEDs is a technique recently developed called imagery analysis. One system that uses this is the Buckeye, which is being developed at the Topographic Engineering Center at the Engineer Research and Development Center within the U.S. Army Corps of Engineers. The Buckeye system consists of a frame camera with an electro-optical sensor, coupled with advanced analysis software to create a very detailed, three dimensional image of a terrain. The whole system is typically mounted on a UAV. The UAV will then repeatedly fly over an area, and compare each pixel to see if any changes have occurred. If overnight, for instance, there appears to be recent digging in a road, a problem area can be flagged and avoided until an explosive disposal team can be dispatched.

Imagery analysis technology would not be applicable for many situations such as areas with limited aerial visibility, but could be very effective against the large buried road bombs. Logistically, it is difficult to monitor large areas, but imagery analysis can be effective in smaller high risk zones and major traffic ways.

Electromagnetic Energy Pulse [3] - This technology, still in development, uses high-power electromagnetic energy to disable the circuitry of IEDs. One system currently being developed is called the Neutralizing Improvised Explosive Devices with Radio Frequency, or NIRF. Ideally this would be a focused electro magnetic pulse that would scan ahead of vehicles and disable any IEDs before they had a chance to detonate, protecting soldiers. This is still not a perfect solution, as it would not be effective against simple IEDs which do not have electronics and only use pressure or trip switches. There is also the possibility that the IEDs could be adapted to shield itself from electro-magnetic waves.

Human Imaging [11] – Although not as widely used as road side IEDs, suicide bombers wearing IEDs are also a threat. Several methods are being developed to see explosives under an individual's clothing. Thermal imaging has been used because any object between a person's body and the camera will block infrared radiation given off by the body from reaching the camera. One problem with this detection technique is that when a person wears an item close to their skin the item's temperature will approach that of the body making it harder to distinguish. Millimeter Wave technology works on similar principles but looks for electromagnetic energy generated between microwaves and long infrared waves that are generated thermally from the body.

2.3 Detection

Protection and prevention are important, but the ideal countermeasure for IEDs would be to detect them for collection and disposal. Detection of IEDs can be broken into two distinct categories: bulk and trace detection. Bulk detection focuses on detecting or seeing the whole device, whereas trace detection looks for evidence that might indicate an explosive is present. These two techniques can be thought of as macroscopic and microscopic, respectively. There are many techniques that have been developed and many more that are being developed. Some of the most common and promising methods are discussed below.

2.3.1 Bulk Detection

X-ray Transmission Imaging [6] - Imaging is one of the most popular bulk detection methods in place. X-ray based screening is still used for airport security. Conventional X-ray transmission based imaging machines work on the principle that photons are absorbed by dense material, but will pass through lighter material. A typical system will have a fan-shaped beam of X-rays and an array of detectors. A target is placed between the two and then the detectors measure the response of the photons, which depend on the attenuation in the sample. This can give a two-dimensional image of the target based on the densities of materials within the target. One of the problems with this system is that depth information is difficult to obtain because the system determines the total attenuation through the sample. Thus, similar results may be obtained for a thin dense material or a thick weak absorber. There is also the problem of an explosive device hidden behind a dense object to mask it. Still, the principles of X-ray physics have been investigated for over a century, which has helped to create relatively inexpensive systems with fairly reliable results.

Dual-Energy X-ray Imaging - These systems are the next generation of X-ray systems and help fix the problem of shadowing objects with dense material. A target is scanned with two beams having different X-ray energies. At lower energies, say below 80 keV, absorption of photons is affected by the average atomic number and the thickness of the material. At higher energies, the photons are less affected by the average atomic number of the material [6]. Comparing the two images, the presence of light elements commonly found in explosives, such as nitrogen, carbon, hydrogen and oxygen, can be detected. This system makes use of the fact that plastic explosives are made of these light elements, but have a density that is between 30-50% higher than most common plastics [7]. While dual-energy systems are a definite improvement on conventional transmission based X-ray systems, they still suffer from some key problems. The system generates an estimate primarily of the densities of the objects in the target, which the operator then has to rapidly interpret. It might be easy to identify a lead shaped teddy bear as inconsistent, but not a laptop constructed from a plastic explosive with a detonator hidden in the computer circuitry.

3D X-ray Imaging [6] - This is another step up the technological ladder for X-ray based imaging. There are several kinds of three dimensional imaging; one of the most common is computed tomography, or CT. This technique was originally developed for medical imaging, but

has since been adapted for many applications such as non-destructive testing and security screening. CT works on the same principle as transmission based radiography. Some CT systems use a dual energy scanning technique to get improved images. These systems typically work by taking multiple "slices" through the object while rotating either the source and detectors around it or the object itself. Responses from all of these "slices" are then used to create a two-dimensional cross-sectional image, through a reconstruction algorithm. CT requires around 100 views from a 1024-element linear X-ray detector in order to produce a 1000 × 1000 pixel slice image. To maintain a high signal to noise ratio, a very high intensity X-ray source is required, which results in a substantial radiation dose to the target. A CT system in service for FAA inspections is the CTX5000, which requires the X-ray scanner to rotate at 15,000 rpm in order to scan a target moving at 0.25 m/s. This method can create extremely detailed three-dimensional images from many two-dimensional images, but the systems are expensive and inspection times are relatively long.

X-ray Fluorescence (XRF) [8] – XRF can be used to get an idea of the composition of a target being scanned. It works by bombarding a molecule with radiation such as X-rays, knocking out an inner shell electron, whose vacant shell is then filled by an outer shell electron. The binding energy for inner shells is more than for outer shells and a photon with a characteristic energy equal to the difference in shell energies is emitted. This is usually more effective for heavy elements having high atomic number (Z), which makes this method more useful at detecting detonators rather then explosives. The main drawback of this technique for IEDs is that it is hard to scan past the surface of a target because of the relatively low energyies of the X-rays given off. An absorbing material surrounding an IED would block both the incident, as well as the generated photons.

Backscatter X-ray Radiography [6] – This technology, based on backscattered X-rays, has improved in recent years. The key difference, as compared to those previously discussed, is that this technology creates an image based on X-rays that scatter back towards the X-ray source instead of those that pass through the target. There are some key advantages of this technique over standard X-ray imaging. Backscattered images are created from the competition between photoelectric absorption and Compton Scattering. The likelihood of a photon undergoing photoelectric absorption rapidly increases with atomic number, whereas the likelihood of Compton scattering is proportional to Z/A, which is fairly constant for most elements, hydrogen

being the biggest exception. Because of this, the image created by backscatter emphasizes low atomic number (Z) materials with high densities. Areas that contain explosives would be expected to show up as light areas. This makes backscatter radiography ideal for detecting common nitrogen-rich explosives. Because of the dependence on atomic number, this technique has also been called Z-Backscatter imaging. This technique however, still suffers from the common flaws found in most imaging techniques. Explosives can still be masked by surrounding them with denser material, and the images require a trained operator to analyze the image making the system only as good as the alertness and skill of the operator. The image is also dependent on the proximity to the target. With its current limited range, this technique would be classified as remote detection. As this technique is still being developed, time will tell if it can be used for true stand-off detection or just remote detection.

PIPAR Imaging [9] – The basis for imaging with photon-induced positron annihilation radiation (PIPAR) is to help get around the limited penetrating ability of X-rays in dense material. Most techniques that use Compton scattering employ photons below 1 MeV because of the reduced chance of Compton interactions taking place for photons of higher energy. PIPAR results when an incident photon of at least 1.022 MeV interacts with an atom and creates an electron and a positron. The positron slows and then annihilates, generating two photons, usually with energies of 511 keV. These 511 keV gamma rays are of relatively high energy, offering them a good chance of escaping the target and reaching the detector. PIPAR reveals something of the composition of the target because the probability of pair-production to occur varies approximately as $Z(Z+A)$ where A is the mass number [9]. This technique has the advantage of interrogating a target deeper than low-energy X-rays, as well as giving clues about the composition. It has the same drawbacks of any imaging system that requires user interpretation.

Neutron Based Interactions [10] – There are several different neutron interactions that can be used by neutron-based explosive detection systems. Some of the main techniques are listed below.

- Thermal Neutron Analysis – TNA uses thermal neutrons to interact with a material and create both prompt and delayed gamma rays.
- Fast Neutron Analysis – FNA uses high energy neutrons to create gamma rays from inelastic scattering reactions.

- FNA/TNA – Uses a pulsed neutron source that creates high energy and thermal energy neutrons for both TNA and FNA.
- Pulsed Fast Neutron Analysis – PFNA uses a neutron source that is pulsed for nanoseconds to generate FNA.
- Associated Particle Imagining – API uses the alpha particle produced in a D-T reaction to indicate the time that a neutron is emitted. The time that a signal is received from, say, an inelastically scattered gamma ray can then be used to indicate the depth at which the inelastic scatter occurred.
- Nuclear Resonant Absorption – NRA uses neutrons over the 0.5 to 4 MeV range to create elastically and resonantly scattered neutrons.

These technologies all work on the same principle of using a neutron source to bombard a target. The neutrons then undergo a variety of interactions within the target, based largely on the neutron energy. By looking for the hydrogen, carbon, nitrogen and oxygen prompt-capture and inelastic-scatter gamma-ray responses, it is possible, in principle, to detect explosives. Neutron-based methods have some key advantages. Neutrons are not stopped easily by dense material so the incoming radiation has a good chance to penetrate into the target. The generated gamma rays usually are of high energy, typically over 1 MeV, which means they stand a better chance of escaping the target and getting back to the detectors. This makes the whole process better at interrogating deeper into a target. These methods also have the advantage of a completely automated analysis that requires no user interpretation.

2.3.2 Trace Detection

Trace detection refers to the identification of explosives from vapors and/or particles given off by explosive compounds. One of the primary problems with vapor detection is the low vapor pressure that some explosives have. This low vapor pressure results in low explosive vapor in the air near a sample. Some examples are EGDN with 64 parts in 10^6, TNT with 6 parts in 10^9, and C-4 with 6 parts in 10^{12} parts of air [11]. These figures illustrate the difficulty of a technology that tries to detect vapor and particles given off by explosives. This method requires a very high degree of efficiency in order to detect the small amounts of vapor in the air. Nonetheless some effective methods have been developed, which are discussed next.

Canine [11] – A tried and true method for detecting explosives has been the use of dogs as explosive vapor detectors. The Department of Defense (DoD) currently has about 1300 dogs with 500 trained to detect explosives. The DoD training program for dogs involves 27 different targets that can be hidden up to 8 feet above the ground or buried up to 3 feet below the ground and the dogs must maintain a 95% success rate. Dogs have some distinct advantages over electronic options. Dogs are very mobile. They can move around a room or building and over rough terrain easily, which remotely operated machines can not. Dogs also have the ability to follow the scent to its source. The vapor plume off an explosive can extend for some distance. When the dogs detect it they will follow the scent cone back to its source locating the explosive for the handler. Although canine training programs for explosive detection usually require over 100 days, the cost is still cheaper than most electronic counterparts. However, dogs have a relatively short duty cycle of 40 to 60 minutes before the animals need a break. The dog's effectiveness is also dependent on the environment and circumstances such as severe weather or noises. Dogs also cannot tell the handler what explosive is found, only that one exists. So while there are many positive aspects of using dogs for explosive detecting, there are also some serious drawbacks that must be considered.

Bugs [12] – Bee olfactory senses are actually more effective than canine's. Some research has been done to use bees in place of dogs. The bees are trained through Pavlovian Conditioning, also known as Classical Conditioning. The bees are exposed to explosive vapor and then given nectar. Over time the bees come to expect the nectar after smelling the explosive and will extend their proboscis in anticipation. By watching the bees' reactions, the presence of explosive vapor can be identified. While bees have a more sensitive olfactory sense, there are several problems with this method. One prototype system puts the bees in a harness with a camera focused on the bee's proboscis. However, the bees typically don't live very long harnessed. One also loses the mobility and the ability to follow an explosive vapor to a source. Although an interesting idea, the feasibility of a technology that uses bees remains uncertain.

Chemical Sensors [11] – There are several technologies that all work on the principle of using electronic sensors to detect the presence of explosive vapors. Chemiluminescence works by electronically exciting NO_2 and then using a photomultiplier tube to detect the light excited by the molecule. Ion Mobility Spectrometry, or IMS, works by ionizing the vapor molecules and then measuring how long they take to drift a set distance. The drift speed depends on the size of

the molecule, and by measuring the drift time, different molecules can be identified. Gas chromatographs use the electronegative property of explosive vapors to identify them from other molecules. There are many more variations of vapor detection techniques that each have their own strengths and weaknesses. The main problem with all of these systems is the low concentration of explosive vapor which results in the detectors having to be very close to the target to be effective. In field conditions the problem is exacerbated with convection currents and wind. While it certainly has its applications, these vapor detection systems will most likely never be able to operate at true standoff distances under outdoor field conditions.

Laser-Induced Breakdown Spectroscopy – This system uses infrared radiation to scan the outside of objects. When the laser comes in contact with residual explosive particles it creates microbursts. The light from these microbursts is characteristic of the explosive involved. Laser trace detection technology has the potential to detect explosives very rapidly, near real-time [6]. This technology also has the potential to detect explosives from as far away as 30 meters [3]. While a very promising technique to look for residual explosive on objects, its inability to scan inside a target will mean a laser system would probably need to work in tandem with another system, perhaps with this neutron interrogation technique as a preliminary filter.

Spot Tests – A cheap and effective way of detecting explosives, swipes or spot tests have been used for years. These work by using chemicals that undergo a color change or some other reaction when interacting with an explosive. Spot tests can be used to help identify which type of explosive is present, but are not available for all explosives [8]. Moreover, as this method requires actual contact with the target, it can only be described as remote detection.

CHAPTER 3 - Present Methodology

Conventional explosives derive their energy from chemical bonds within compounds. When these compounds are exposed to enough heat, shock or electrical charge they quickly rearrange their molecular structure, breaking down into reaction products. Some of the energy that was used to hold the molecules together is released, as well as energy from the formation of reaction products. Most common explosives fall into the category of nitrogen-rich explosives. The reason for this is because of the chemical properties of nitrogen. Nitrogen gas is one of the most stable compounds on the planet with a triple bond between the two nitrogen atoms. When one mole of nitrogen atoms bond, 960 kJ are given off. The more nitrogen atoms present in an explosive, the more free nitrogen atoms available when the substance begins to break down and the more energy given off by the formation of nitrogen gas. This is why most common explosives are called nitrogen-based and have an unusually high fraction of nitrogen atoms. The levels of hydrogen, carbon, nitrogen, and oxygen in these explosives are unique and can be used to distinguish them from other materials. Not all explosives are nitrogen-rich but it is fair to say the nitrogen-rich explosives are the most common world wide. Figure 3.1 illustrates that a window exists within which most nitrogen rich explosives are distinguished from other materials based are their ratio of nitrogen and oxygen. Figure 3.2 provides another example of the unique elemental composition of explosives compared to other materials.

Knowing the approximate chemical composition of explosives is an important first step to identifying them. The signature-based radiation scanning method involves the active interrogation of a target with neutrons, causing atomic interactions that generate a set of responses or signatures. These interactions produce characteristic responses that allow for identification of the composition of a target by comparing the responses from the target with those from a typical explosive. There are three neutron interactions that are considered to generate gamma ray and neutron responses.

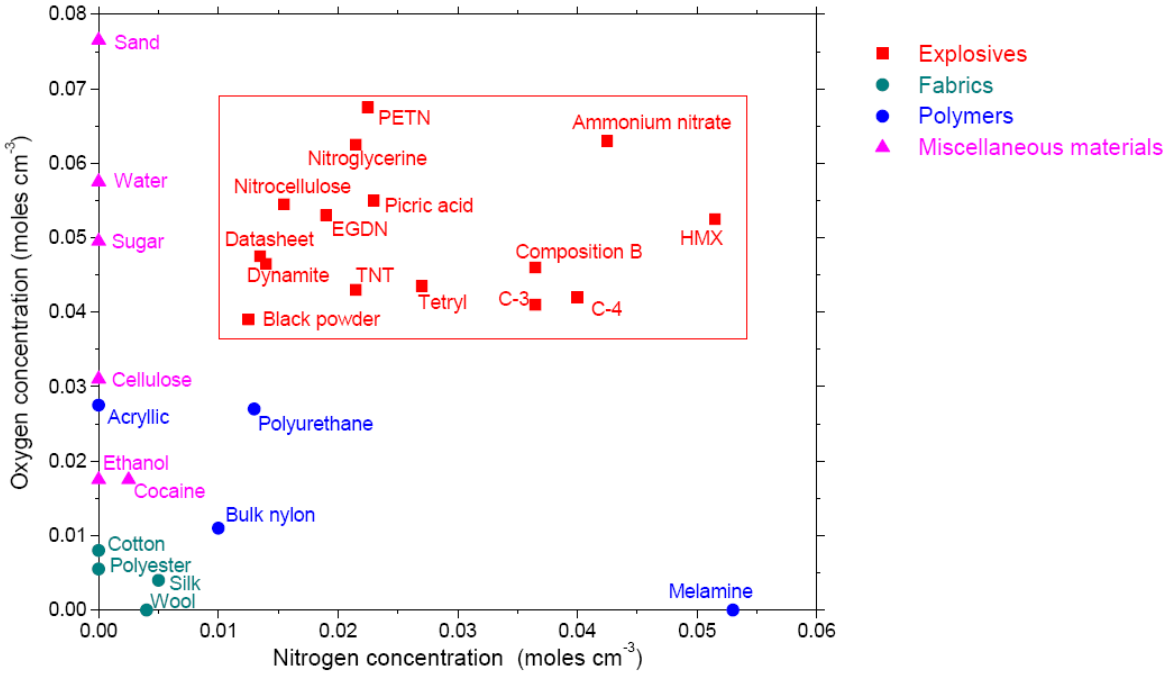

Figure 3.1. Explosive compositions, with respect to oxygen and nitrogen concentrations, compared to some inert materials [14].

3.1 Prompt Neutron Capture

Since a neutron has an electrical charge of zero, its kinetic energy is not affected as the neutron approaches a nucleus. Neutrons of any energy can cause nuclear reactions as they are not affected by the Coulomb-barrier. It is more likely, however, for low energy neutrons to undergo radiative capture or the (n, γ) reaction. Neutrons can be broken into several groups. Fast neutrons are generally considered to have energy greater then 1 MeV. Epithermal neutrons are generally considered to have energy between about 0.2 eV and 1 MeV. Thermal neutrons are defined to have an energy of less then 200 meV. The most probable energy of neutrons in thermal equilibrium with a medium whose temperature is 293 k is around 0.025 eV. Thermal neutrons can also be characterized by their most probable speed (2198 m/s) or energy (4×10^{21} J) [13].

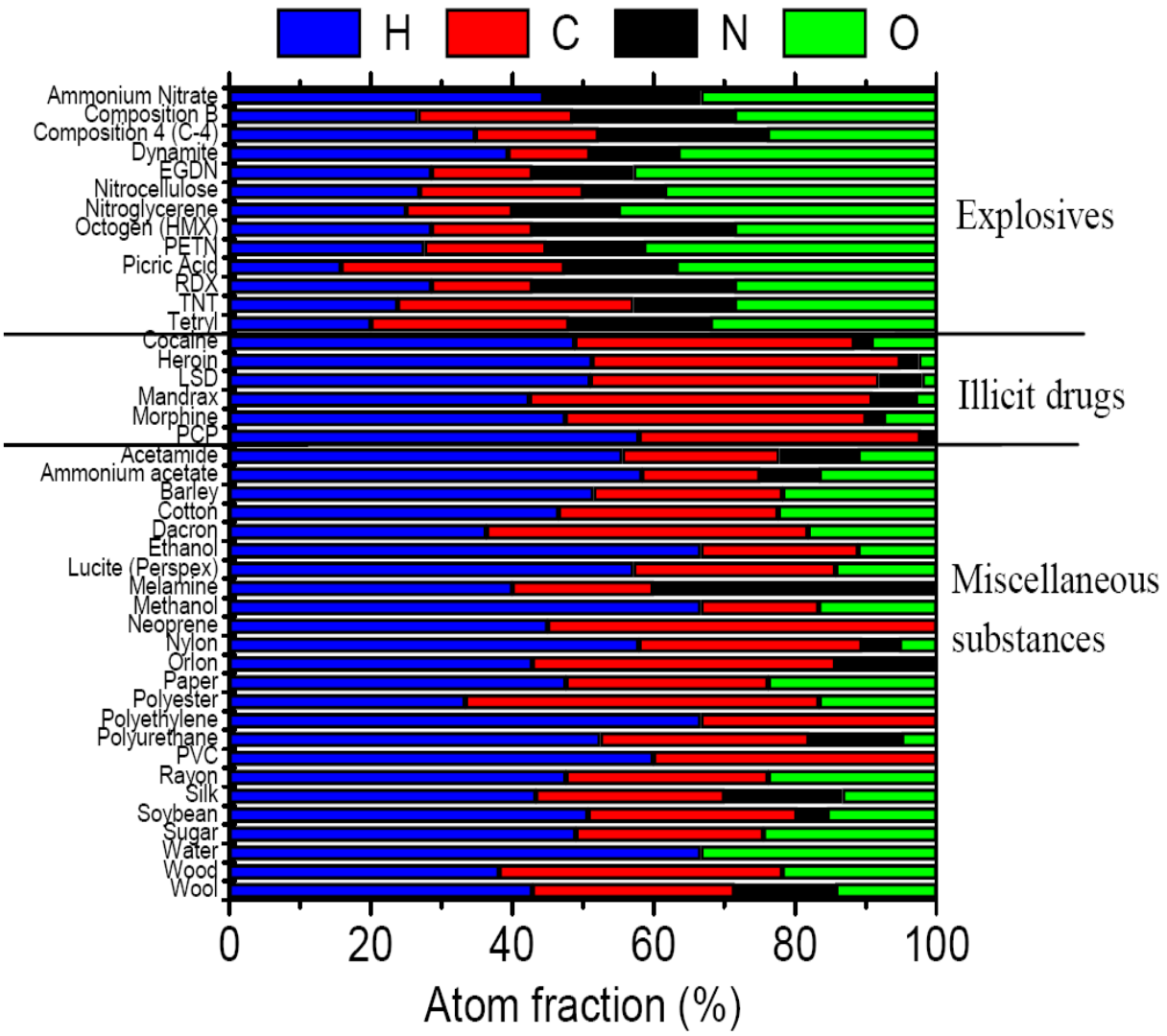

Figure 3.2. Compositions of some explosives and some benign HCNO materials [14].

Radiative capture involves a nucleus absorbing a neutron and a compound nucleus being formed. This nucleus is in an excited state, which decays to the ground state by gamma-ray emission. This reaction is often referred to as prompt capture because the nucleus usually decays in around 10^{-16} s. It does so by emitting one or more gamma rays in a cascade. These prompt-capture gamma rays have characteristic energies, which can be used to identify the isotope from which the gamma ray was emitted [13].

The probability of this interaction taking place is defined by its cross section which has units of barns (1 barn is equivalent to 10^{-28} m^2). This capture cross section is largely a factor of the incident neutron energy. This can be modeled by the 1/v law which means the cross section

and the velocity of the neutrons are inversely proportional. Most tables of prompt gamma-ray energies are tabulated for 2200 m/s neutrons [13]. The energies generated from 2200 m s^{-1} neutrons for the predominant peaks generated from hydrogen, carbon, nitrogen, and oxygen are listed in Table 3.1. It was discovered early in the project that most of the prompt gamma rays were not useful because the cross sections were too small to distinguish them from the background radiation. In the end, only the 2.223 MeV capture gamma ray from hydrogen, the 1.262 MeV capture gamma ray from carbon, the 0.871 MeV capture gamma ray from oxygen, and the 10.829 MeV gamma ray from nitrogen were used. Although the efficiency of the detectors was very low for the 10.829 MeV gamma ray, the lack of competing signatures at the energy range made it viable. A list of prompt gamma rays and their cross sections can be seen in the following table. All prompt-capture gamma rays are listed for carbon, hydrogen and oxygen but only the most probable are listed for Nitrogen, as there are more than 60 prompt-capture gammas for this element.

Table 3.1. Table of thermal capture gamma-ray energies for hydrogen, carbon, nitrogen, and oxygen [20].

Element	Energy (keV)	σ(barns)	Element	Energy (keV)	σ(barns)
Hydrogen	**2223.248**	**0.3326**	Nitrogen	5269.159	0.0236
Carbon	**1261.765**	**0.00124**	Nitrogen	5297.821	0.0168
Carbon	3683.92	0.00122	Nitrogen	5533.395	0.0155
Carbon	4945.301	0.00261	Nitrogen	5562.057	0.0084
Nitrogen	1678.281	0.0063	Nitrogen	6322.428	0.0145
Nitrogen	1681.24	0.00129	Nitrogen	7298.983	0.00746
Nitrogen	1884.821	0.0147	Nitrogen	8310.161	0.0033
Nitrogen	1999.69	0.00323	Nitrogen	9148.98	0.00129
Nitrogen	2520.457	0.00441	**Nitrogen**	**10829.12**	**0.0113**
Nitrogen	2830.789	0.00134	**Oxygen**	**870.68**	**1.77E-04**
Nitrogen	3531.981	0.0071	Oxygen	1087.75	1.58E-04
Nitrogen	3677.732	0.0115	Oxygen	2184.42	1.64E-04
Nitrogen	4508.731	0.0132	Oxygen	3272.02	3.53E-05

3.2 Inelastically Scattered Gamma Rays

Inelastic scattering of neutrons is also known as the (*n*, *n*') reaction. Inelastic scattering is a form of capture scattering in which an incident neutron is absorbed by the scattering nucleus

which then forms a compound nucleus. The compound nucleus decays by emission of a neutron and the residual nucleus is left in an excited state in inelastic scattering [22]. The excited nucleus then returns to ground state by emission of a gamma ray of energy equal to the change in the quantum state of the nucleus. This reaction can only occur when the neutron incident on a nucleus has energy above the threshold energy of the first excited state of the scattering nucleus [13]. The threshold energy E_t, for inelastic scattering to take place is given by

$$E_t = -\frac{A+1}{A}Q, \tag{1}$$

where A is the atomic mass of the target nucleus and Q is the Q value of the reaction. The Q value is unique for each state to which the nucleus is excited. The larger the nucleus, the more quantum states, and therefore the more inelastically scattered gamma rays can be generated. Plots of the cross sections for the possible gamma rays that can be generated, for different excited states, for carbon, nitrogen and oxygen are given in Figs. 3.3 – 3.5.

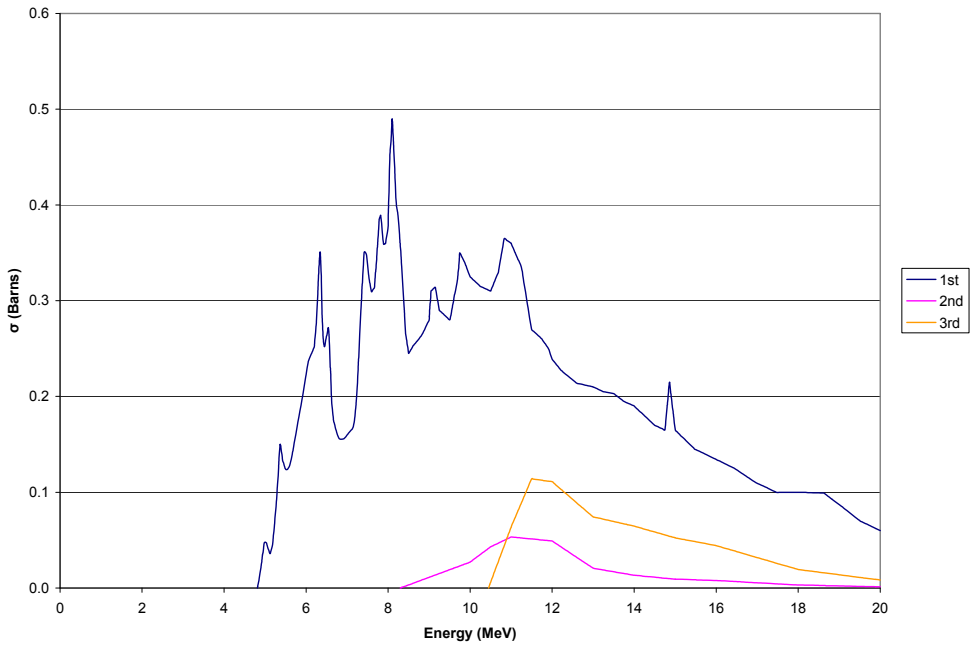

Figure 3.3. The inelastic gamma-ray cross sections for carbon, as functions of neutron energy [generated from MCNP5].

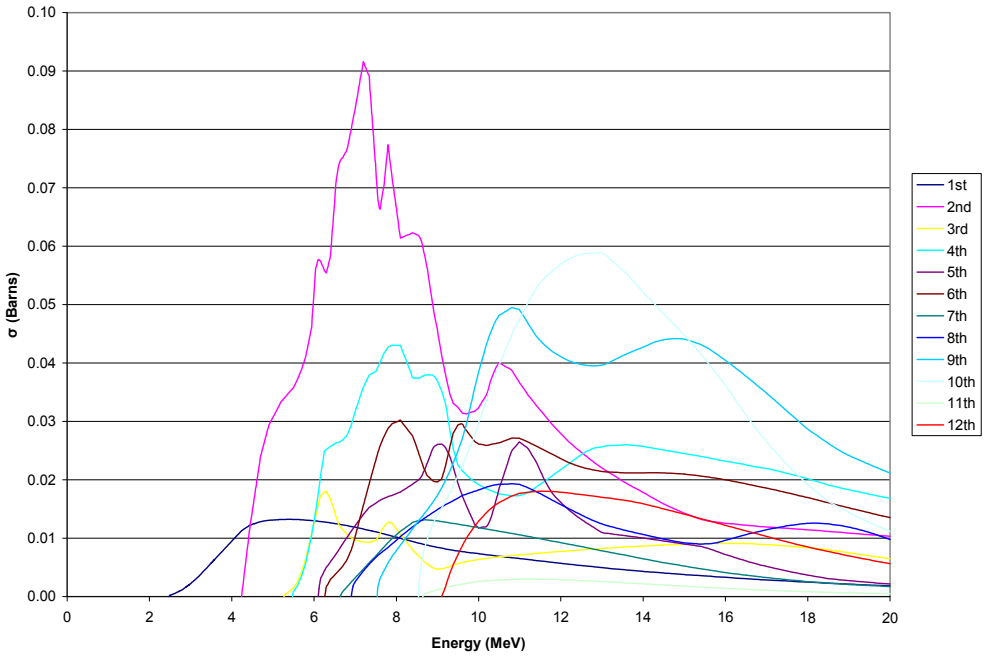

Figure 3.4. The inelastic gamma-ray cross sections for nitrogen, as functions of neutron energy [taken from the National Nuclear Data Center].

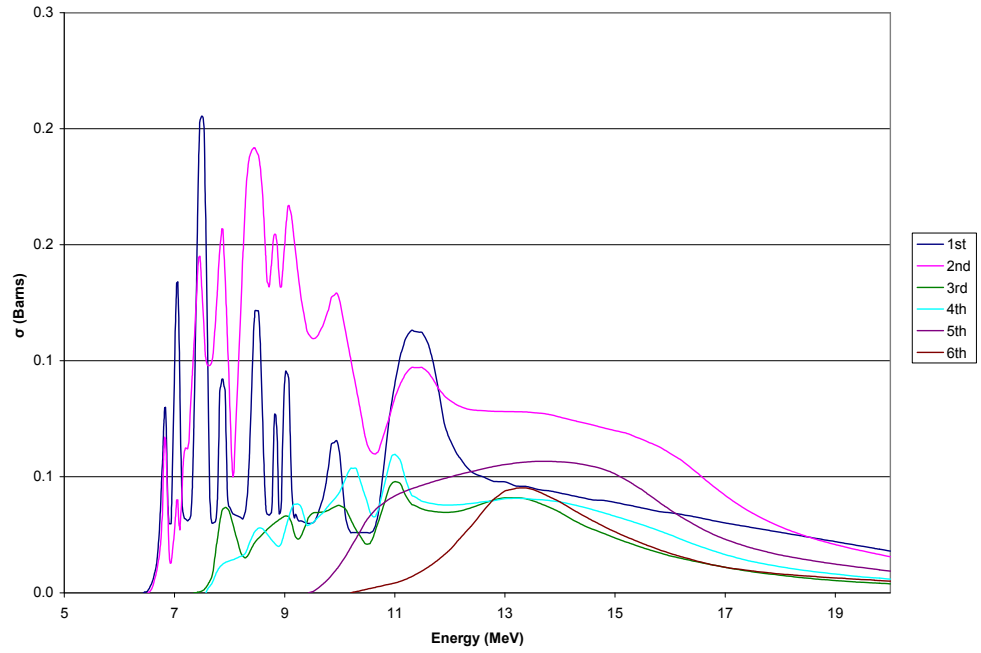

Figure 3.5. The inelastic gamma-ray cross sections for oxygen, as functions of neutron energy [taken from the National Nuclear Data Center].

It is clear that the probability of the interaction varies with energy, and there may be a low probability for the reaction to occur even if the neutron has an energy above the threshold energy required for the reaction.

3.3 Thermalization

As neutrons move through material they collide with atoms and lose energy through elastic scattering. The ratio of the final (E_f) and initial (E_i) kinetic energies of a neutron in the LAB frame of view is given by

$$\frac{E_f}{E_i} = \frac{A^2 + 2A\cos\theta^* + 1}{(1+A)^2}. \tag{2}$$

In this equation θ^* is the scattering angle and A is the mass of the scattering nucleus. From this equation it can be seen that the maximum energy loss occurs with a nucleus of similar size to a neutron. That is why hydrogen makes the most effective moderator of neutrons. By measuring the ratio of backscattered thermalized neutrons, a gage of hydrogen content can be estimated.

The actual thermal neutron count was recorded by using two LiI(Eu) scintillating neutron detectors. One was covered in a 1mm sheet of cadmium, which filters thermal neutrons because of its enormous thermal neutron absorption cross section. This resulted in one detector detecting both fast and thermal neutrons, and the other detecting only fast neutrons.

3.4 Gamma Ray Detection

The gamma rays themselves presented their own problems for detection as they were of much higher energy than those usually detected in spectroscopy. The problem with detecting high energy gamma rays is that they rarely deposit all of their energy in the detector before escaping. There is a limited active region in a HPGe detector and if the gamma ray escapes before depositing all of its energy, then the full energy of the gamma ray will not be counted. Figure 3.6 shows how the efficiency of a 15% efficient HPGe detector decreases with respect to incident gamma-ray energy. It can be seen that the efficiency of this detector drops by orders of magnitude between 100 keV and 10 MeV. This makes the high energy gamma rays, like the 10.829 MeV prompt-capture gamma ray from nitrogen, difficult to measure because if thousands of gamma rays make it to the detector, only a few will be counted. However, the trade-off is that there are few competing gamma rays at those high energies to mask the signature.

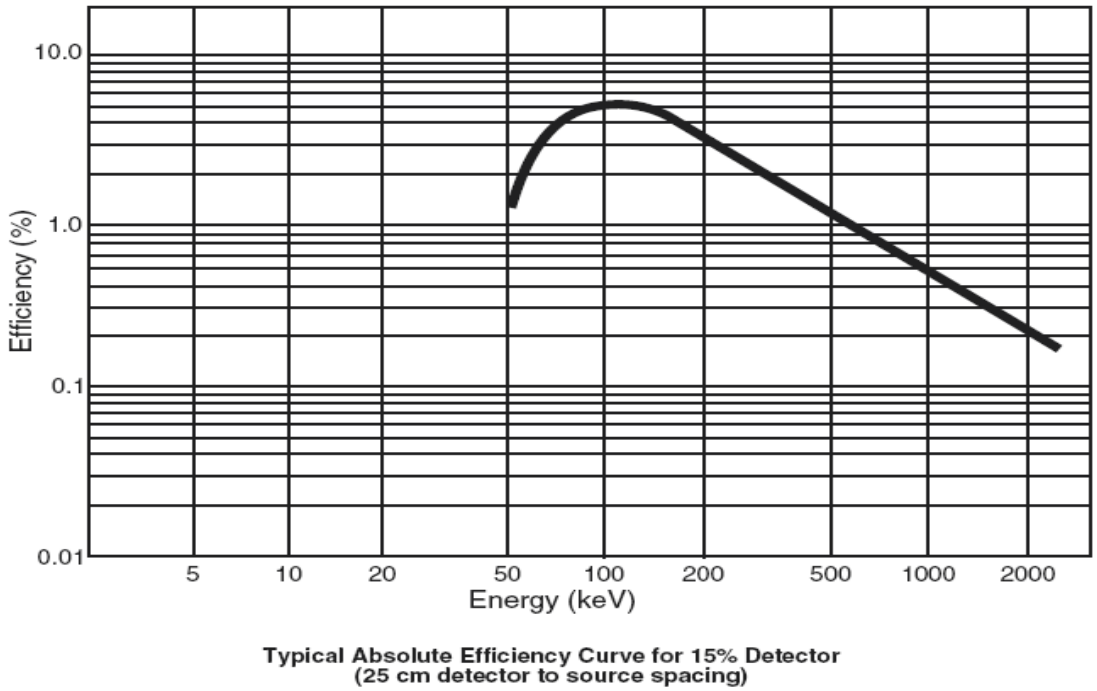

Figure 3.6. Graph of 15% efficient HPGe detector with respect to energy (keV) [21].

CHAPTER 4 - Experiments

4.1 Setup

A 20% efficient Canberra high purity germanium (HPGe) detector (model GC2019) was used to collect the gamma-ray spectra. This detector was connected to a Canberra InSpector 2000 MCA (Model IN2k), which was connected to a laptop computer that used Genie 2000 spectroscopy software. The net peak areas for each of the gamma-ray signatures were estimated using the region-of-interest (ROI) function of Genie. This was accomplished by placing ROI points on each side of a peak. The software then determined the total integral and baseline continuum within the ROI. The total integral T was simply solved for by summing all of the counts within the ROI. The baseline continuum B was estimated as the number of counts within a trapezoid bounded by the ROI end points and a straight-line fit between the ROI end points (the gray area in Fig. 4.1). (This is also the area of a rectangle of width W and appropriate height H, as also shown in Fig. 4.1.) Then the net peak area N was solved for by subtracting the baseline continuum from the total integral, i.e.

$$N = T - B \,. \tag{3}$$

The standard deviation of the net peak area also was given by the Genie software. In principle, this can be estimated using the propagation of errors formula

$$\sigma(N) = \left[\left(\frac{\partial N}{\partial T} \right)^2 \sigma^2(T) + \left(\frac{\partial N}{\partial B} \right)^2 \sigma^2(B) \right]^{1/2}, \tag{4a}$$

which reduces to

$$\sigma(N) = \left[\sigma^2(T) + \sigma^2(B) \right]^{1/2}, \tag{4b}$$

where $\sigma^2(T) = T$ is the variance in the total integral and $\sigma^2(B)$ is the variance in the baseline continuum.

Two Lil(Eu) scintillation neutron detectors (Model 25B3), one cadmium covered, were used to find two neutron scatter signatures. They were connected to Spechtech neutron counters (Model ST 360), which then were connected to the laptop. Figure 4.2 shows a schematic of the equipment used.

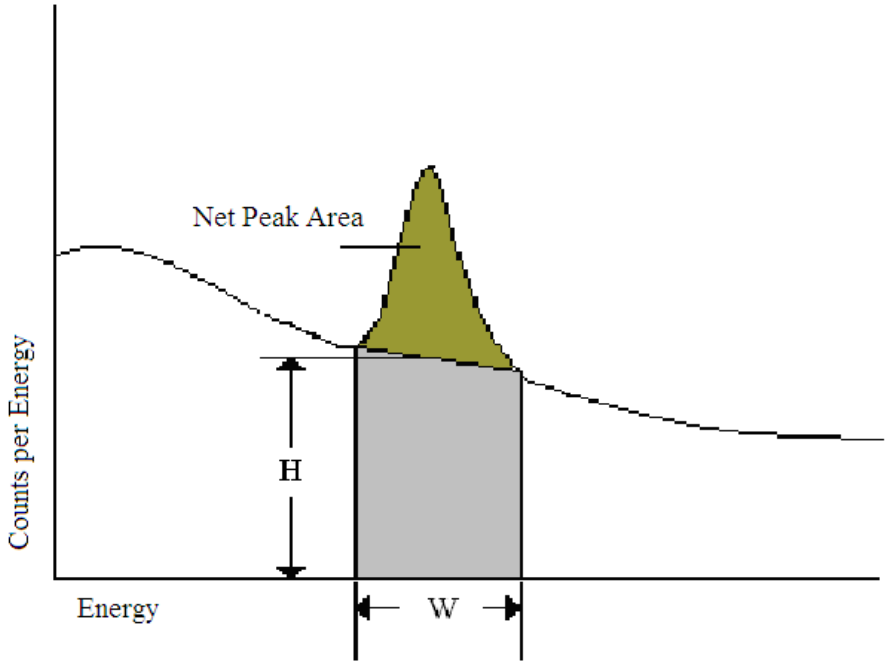

Figure 4.1. Example of net peak area.

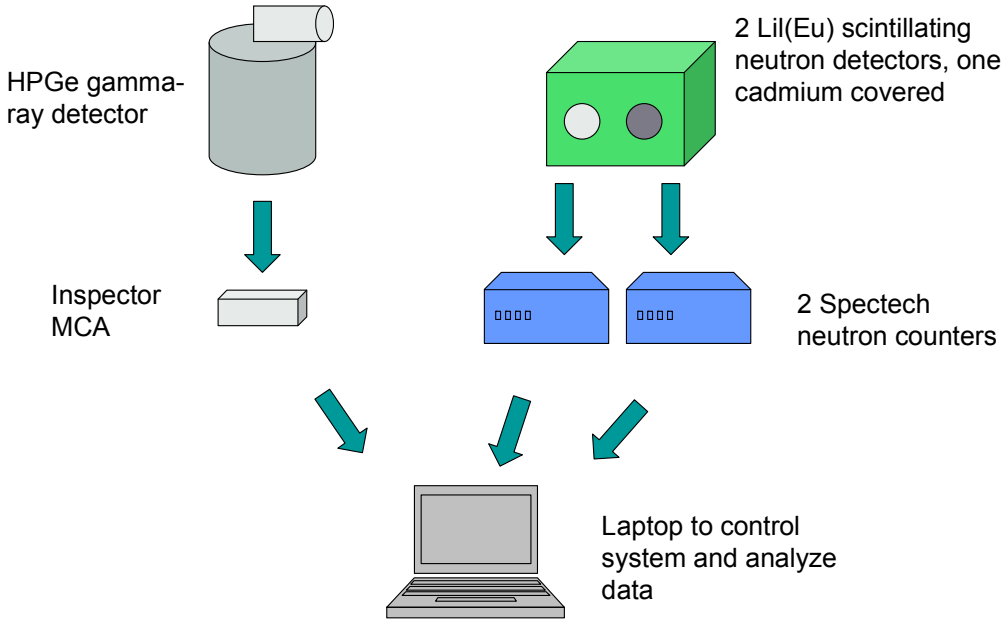

Figure 4.2. A schematic of the radiation detection equipment used in the experiments.

The first step in conducting the experiments was calibrating the HPGe detector. Most calibrations are done with check sources that emit decay gamma rays at known energies. That was not sufficient for these experiments because decay gamma rays rarely have energies above 1 MeV. As an energy spectrum of up to 11 MeV was needed, the system would have to extrapolate the remaining range so a multi-stage calibration was used. First, check sources were used to determine the high-voltage and gain needed to have the multi-channel analyzer's (MCA) channels cover the desired energy range. Once that was done, a preliminary calibration was done with check sources. This was a close enough calibration that then allowed for the identification of higher energy gamma rays. Prompt gamma rays given off from a $NaCl_2$ salt block were used to generate the high-energy gamma rays needed. Figure 4.3 is an example of a typical collected spectrum. This spectrum was collected from the $NaCl_2$ block with the highlighted peaks being those used in the calibration.

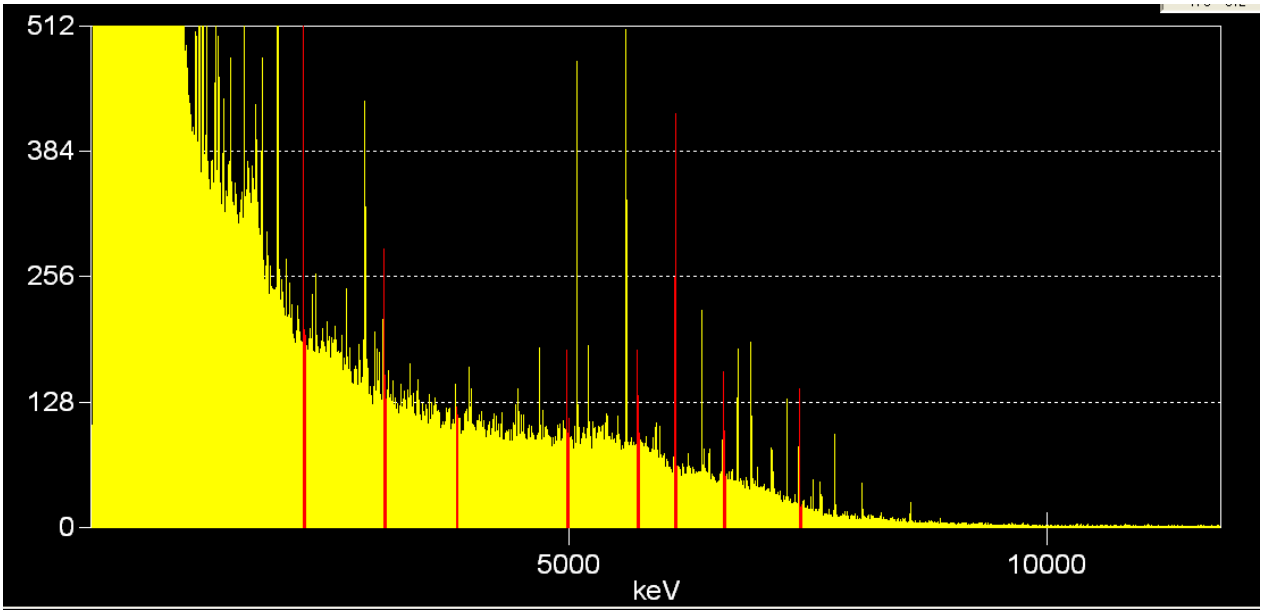

Figure 4.3. Example spectrum.

There are many peaks collected during an interrogation; some of which are within a few keV of each other, making it difficult to identify which peaks belong to which elements. Thus, it is important to have a precise calibration of the detection system. After collecting the channel numbers that each of the known calibration peaks were centered on, a linear calibration could be performed. An example of this can be seen in Figure 4.4.

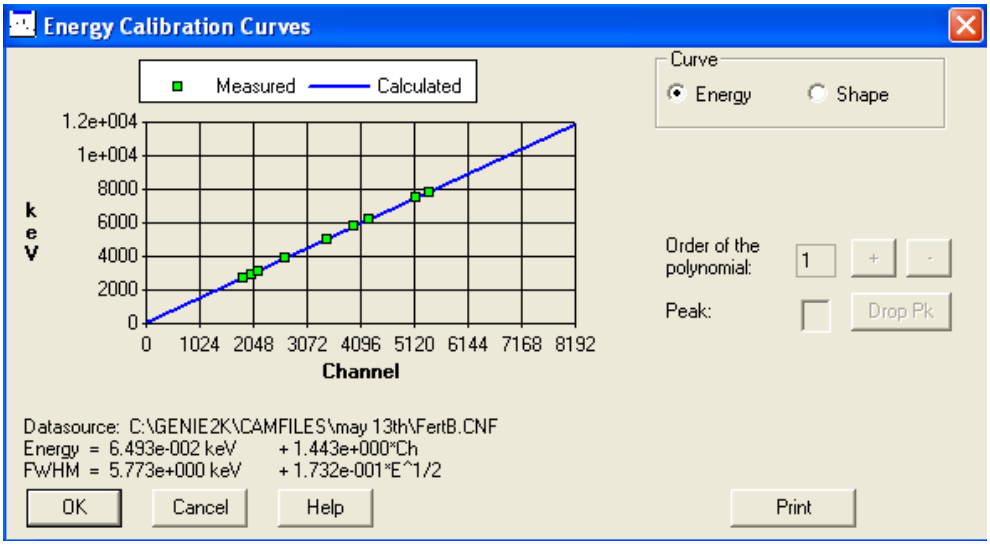

Figure 4.4. Example of calibration.

The large number of detectable chlorine prompt gamma rays was useful in generating a good calibration line that minimized extrapolation by the system.

4.2 Reactor Based Experiments

For the majority of the experiments, the tangential beam port of the Triga Mk II nuclear reactor at Kansas State University was used as a neutron source. This neutron source had advantages and disadvantages. The reactor produces a relatively high flux of about 10^6 n cm^{-2} s^{-1} at 50 cm from the outer wall of the tangential beam port. The beam port also produces a highly collimated beam, which is useful for interrogating smaller samples and reduces background in the collected spectra. The width of the beam was measured using a neutron detector and taking a 1 minute count in 1 inch increments across the front of the target. It was discovered that at 3 meters from the bioshield wall of the reactor, the beam width was around 5 inches as can be seen in Figure 4.5. The tangential beam port also had a much lower gamma background than other beam ports.

The disadvantages are that the ^{235}U fission spectrum produces relatively few high energy neutrons, which are required to excite some of the inelastic-scatter gamma rays. The most probable neutron energy from the fission of ^{235}U is 0.7 MeV with an average energy of 2.1 MeV [8]. Figure 4.5 shows a thermal fission spectrum from ^{235}U and a spontaneous fission spectrum from ^{252}Cf.

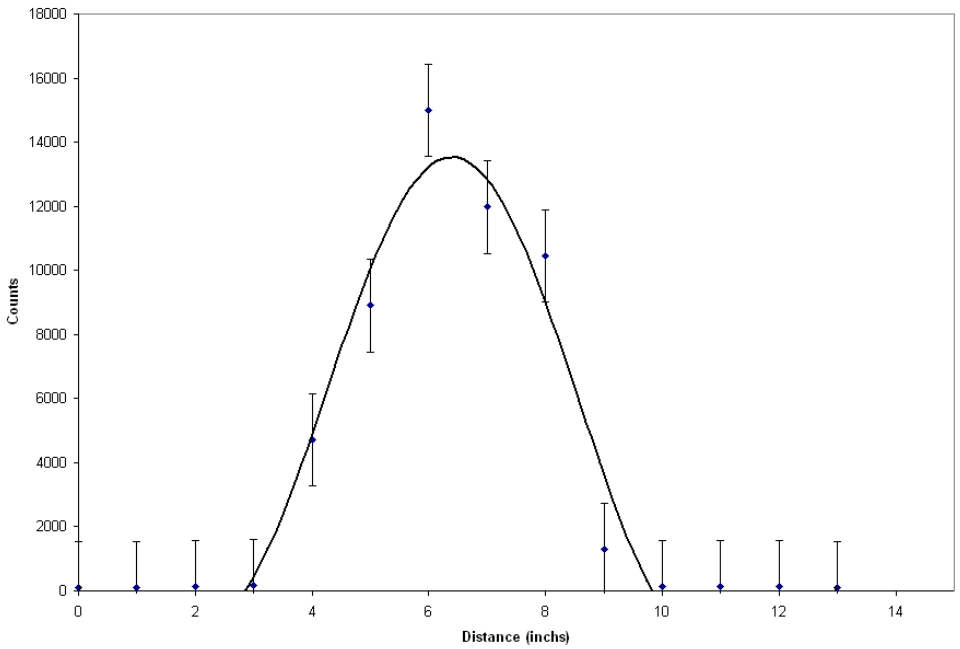

Figure 4.5. Beam width of S.E. beam port neutron beam of K-State Triga Reactor at 3 m from bioshield.

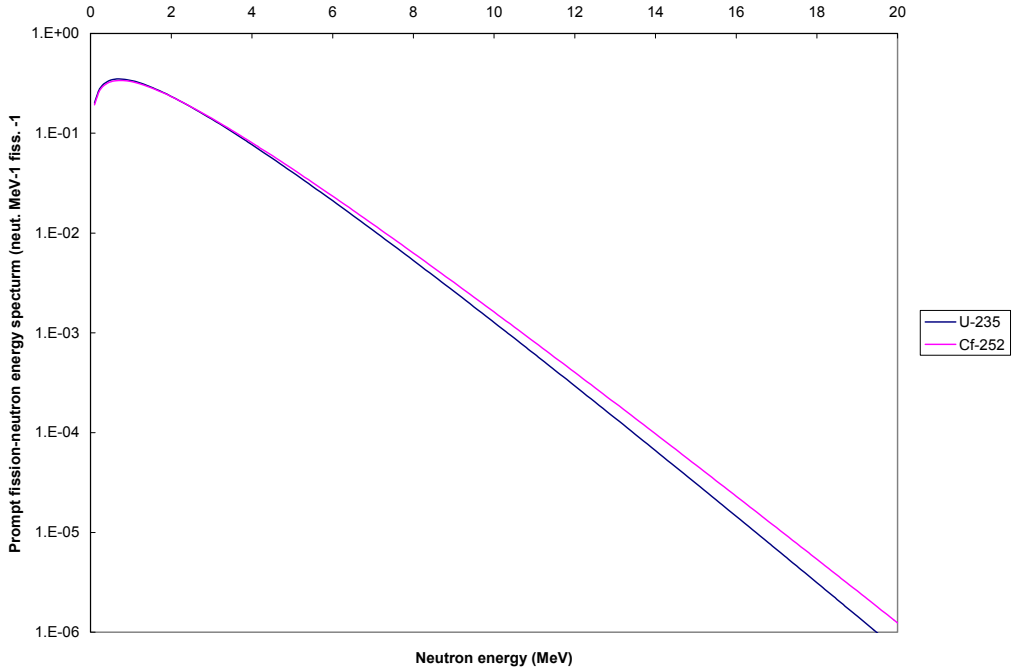

Figure 4.6. Energy spectrum of prompt neutrons produced from U-235 and Cf-252 as calculated by Walsh [1989].

In addition to the already few high-energy neutrons, the fact that the thermal beam port was tangential to the reactor meant that only scattered neutrons were in the beam, further reducing the average neutron energy. It was necessary to use this beam port, however, as the gamma-ray background would be too high from the other three beam ports. The reactor is also a fixed facility and thus is not a suitable neutron source for a field system.

For these experiments, 3.8-L (one gallon) cans were filled with several different materials. Fertilizers were used to simulate explosives. The first (FertA) contained 30% N, the second (FertB) contained 36% N, and the third (FertAB) was a 50-50 mixture of the two. In one experiment, ammonium nitrate was used as a fourth explosive surrogate. Inert materials included sand, chalk, aluminum, plastic, water, rubber, and an empty can. The containers were placed inside a suitcase 2.5 meters from the end of the beam-tube shutter. The HPGe detector was placed on the same side as the reactor and was over a meter from the suitcase. A diagram of the experimental layout for the reactor experiments is shown in Figure 4.7. The experiments were performed by first bringing the reactor up to power, usually 500 kW. The tangential beam port had a shutter in front of it that when closed allowed for a safe working environment so samples could be changed without having to shut down the reactor. The shutter was opened and a spectrum was collected, then the shutter was closed, the samples changed, and the process repeated. Two photographs of the experimental arrangement are provided in Figs. 4.8 and 4.9.

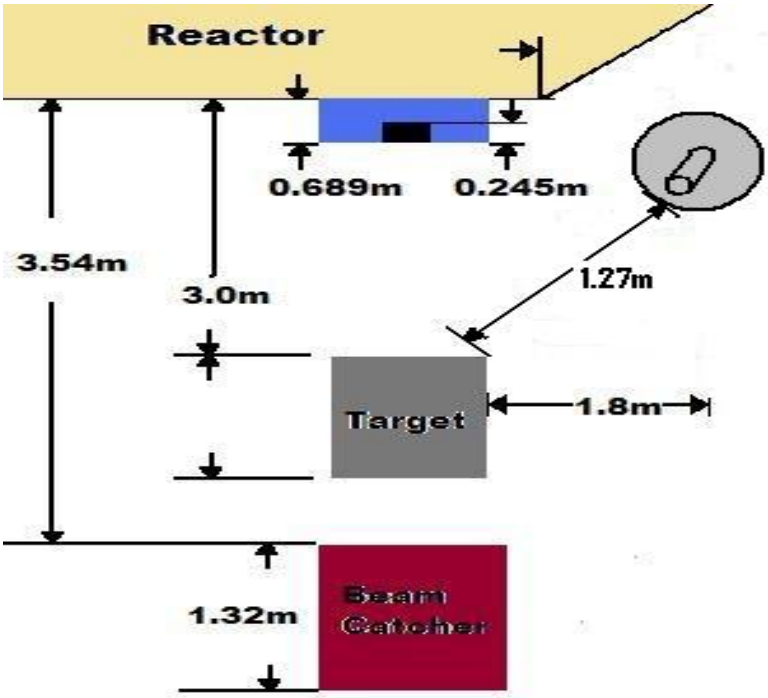

Figure 4.7. Diagram of the experimental layout for the reactor experiments.

Figure 4.8. Suitcase with sample.

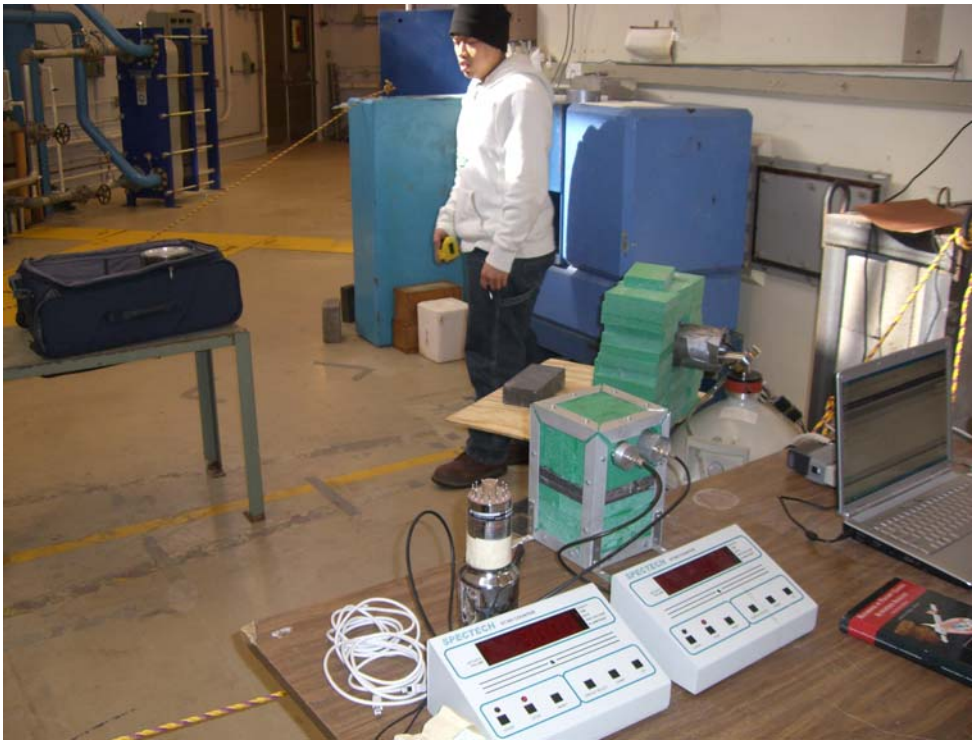

Figure 4.9. Overview of experiment.

4.3 Californium Based Experiments

In an attempt to move towards a working prototype, as well as use more inelastic gamma-ray signatures, a Californium-252 source was used. Approximately 3% of the radioactive decay from ^{252}Cf occurs by spontaneous fission. The ^{252}Cf source at Kansas State University weighed 1.157 x 10^{-5} grams in May 2008. Since 1 microgram of Cf-252 emits 2.314 x 10^{6} n/s, this gave the activity of the source to be approximately 3 x 10^{6} n/s and the uncollided flux at 140 cm from the source was estimated to be 14 n cm^{-2} s^{-1}. The ^{252}Cf source produces neutrons that have a probable energy of 0.75 MeV and an average energy of 2.1 MeV [17]. The fission spectrum from Cf-252 can be modeled by a Watt distribution, like ^{235}U, but it is slightly shifted to a higher energy as shown in Fig 4.6. Although a 50 keV increase in probable neutron energy was not significant over the U-235 spectrum, it was presumed to be a significant increase over the spectrum from scattered neutrons at the exit of the tangential beam port.

The Cf-252 source had only been used for calibrations in the past and was not collimated. This required the construction of a collimator that would focus the beam at the target, as well as shield the surrounding area from the source. The material used for the collimator was 5% borated polyethylene and the radiation simulation program, MCNP5, was used to find the

required thickness to have the dose at the outer wall of the collimator be less then 2 mrem per hour. A typical MCNP5 input dataset for one of these simulations is provided in the Appendis. A schematic of the cross section of the collimator can be seen in Figure 4.10. It was a 26 inch cube that was placed on top of the ^{252}Cf source with a 2 inch square beam tube that was 12 inches long to collimate the neutrons. The construction of the collimator used stair stepped pieces to prevent neutron streaming through spaces. After construction, the dose rates were measured at all sides to be approximately 1.8 mrem per hour. The beam width at the target was also measured using the same process done with the reactor and was found to be around 20 inches wide with the results shown in Figure 4.11. This large beam width was expected considering the relatively short collimator length. A picture of the partially assembled collimator is show in Figure 4.12.

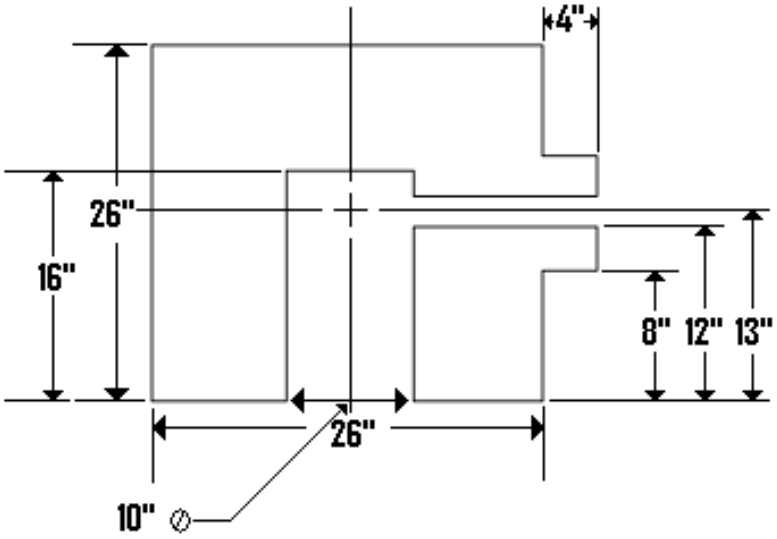

Figure 4.10. Cross-section schematic of californium collimator.

A similar setup with the same equipment was used with the Californium-252 source as the neutron source. Several experiments were performed using the same procedure as the reactor experiments. It was hoped that even with the lower flux of the ^{252}Cf, the advantage of higher average neutron energy would produce superior results. However, the hardened neutron spectrum of Californium did not produce improved results due to the relatively low flux at the target. Longer count times were collected, up to 24 hours, but no new inelastic gamma rays were detected.

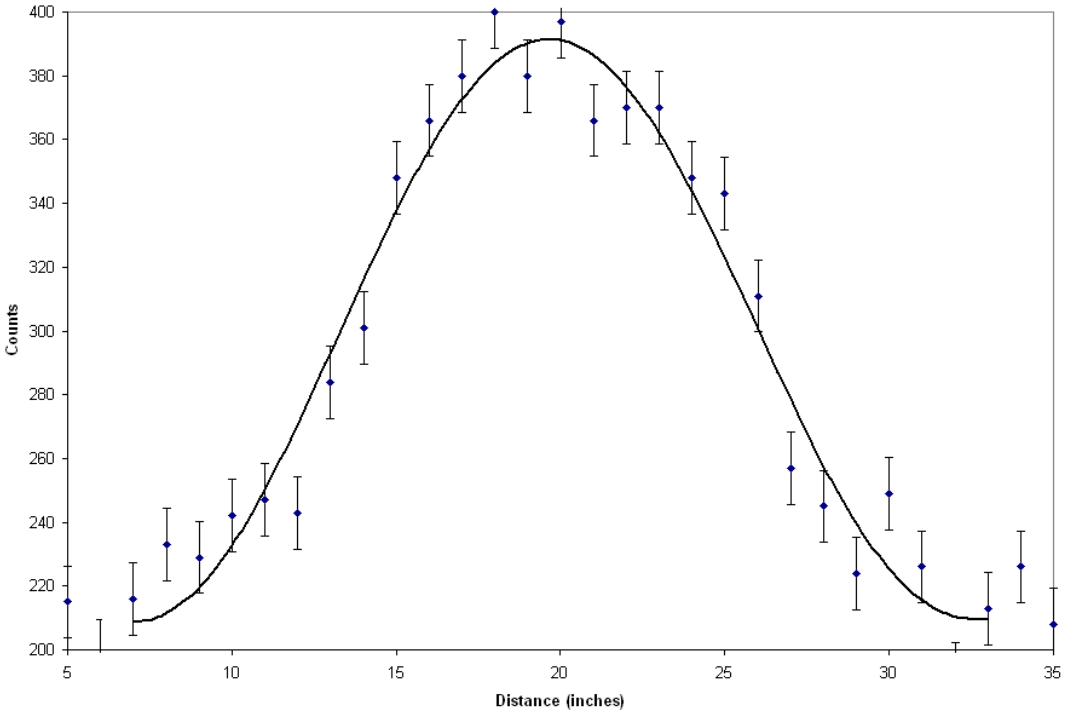

Figure 4.11. Neutron detector response profile 1 m in front of the Cf-252 collimator.

Figure 4.12. Cf-252 collimator during its construction.

CHAPTER 5 - Analysis and Results

5.1 Overview of SBRS

The SBRS method to detect IEDs is unique in that it does not seek to quantitatively analyze or to image a target, but rather employs template matching. The only goal is to identify if the target contains an explosive. This is done by looking at the responses that come back from a scanned target. The target responses are then compared to the responses that would be present if an explosive were present. A figure-of-merit and its standard deviation are used to form filter functions, which are compared to a cut off value that differentiates safe materials from explosive materials. Ultimately, the SBRS method will use a combination of neutron and photon induced responses as well as other possible signatures such as the weight of a vehicle. For the neutron induced signatures, after much experimentation, the five gamma-ray signatures in Table 5.1 were used to differentiate explosive-surrogate samples from inert samples.

Table 5.1. Signatures used in analysis.

Signature Number	Energy (MeV)	Source
1	0.871	Oxygen Capture
2	1.262	Carbon Capture
3	2.223	Hydrogen Capture
4	2.31	Nitrogen Inelastic Scatter
5	10.829	Nitrogen Capture

Originally, neutron thermalization signatures were intended to be used. It was found, however, after experimentation that these signatures were not as useful as expected due to repeatability problems. The data collected from the two neutron detectors for two experiments are shown in Table 5.2, where detector 1 was bare and detector 2 was cadmium covered. The experiments were not conducted for the same amount of time. It was expected, however, that when the samples were compared to each other, for each experiment, they would have a similar ranking. An example can be seen by looking at the results from detector two for FertA, which had the most counts of any sample in experiment one, but was third highest in Experiment 2. The most likely explanation for this is that neutron scattering takes place inside and outside of the target and scattering in the 1 gallon samples might have ultimately represented a small

amount of the total scattering the neutrons underwent. Therefore neutron scattering in the samples contributed only slightly to the total signature, resulting in the poor differentiation among samples. It was decided that the 2.223 MeV prompt gamma ray was a better, more reliable indication of hydrogen content and the neutron signatures thus were not used in the analysis of results.

Table 5.2. Neutron detector counts for two experiments.

Experiment 1		Experiment 2	
Detector 1		Detector 1	
Rubber	688460	Sand	193620
FertB	679042	Rubber	193588
FertA	677813	FertA	189764
Water	675136	FertB	189459
Sand	658116	Water	182169
Detector 2		Detector 2	
FertA	121416	Rubber	121974
Rubber	119961	FertB	95198
FertB	118395	FertA	93647
Water	117410	Sand	82171
Sand	116009	Water	50601

5.2 Template Matching Procedure

A template-matching technique is used that compares the vector **R** of N signatures from an unknown target to a template $\mathbf{S}_\ell$, which is a vector of signatures from a similar target known to have explosives present, for each of $\ell = 1, 2, \ldots, L$ configurations of the target. The presence of a chemical explosive is detected if the vector **R** matches any one of the templates to a sufficient degree. If there is no match, the target is presumed not to be explosive.

A neutron beam is used to interrogate a target from some standoff distance. A detector capable of energy discrimination records a spectrum from which several signatures are estimated. Each signature is the net number of counts under a peak from a capture or inelastic-scatter gamma ray from hydrogen, carbon, nitrogen, or oxygen. A figure-of-merit (FOM) of the following form is generated [19]

$$\zeta_\ell = \sum_{i=1}^{N} \alpha_i \frac{\left(\beta R_i - S_{i\ell}\right)^2}{\beta^2 \sigma^2\left(R_i\right) + \sigma^2\left(S_{i\ell}\right)},\ \ell = 1, 2, \ldots, L, \tag{5}$$

In Eq. (5), ℓ refers to a particular template among the total number L of templates in the library. The α_i is a weight factor for the i^{th} signature. This allows tuning of the FOM to maximize the distinction between inert and explosive material by giving some signatures more importance and some less. The weight factors are scaled so that $\sum_{i=1}^{N} \alpha_i = 1$, β is a factor that scales the measured signatures to the templates. This will allow templates that were collected for different amounts of time to be compared. σ^2 (R_i) is the variance of the measured responses and σ^2(S_{il}) is the variance of the template response. These variances are automatically calculated by the Genie software which collects the data and given with the net area of the signature's peak. An estimate of the standard deviation of the figure-of-merit is given below [19]

$$\sigma\left(\zeta_\ell\right) = 2\left[\sum_{i=1}^{N} \alpha_i^2 \frac{\left(\beta R_i - S_{i\ell}\right)^2}{\beta^2 \sigma^2\left(R_i\right) + \sigma^2\left(S_{i\ell}\right)}\right]^{1/2}. \tag{6}$$

Equations (5) and (6) are used to define the filter functions

$$f_\pm\left(\lambda\right) = \zeta_\ell \pm \lambda\sigma\left(\zeta_\ell\right), \tag{7}$$

where λ is a constant. The value of λ establishes the confidence value of the system and is set by the user. If ζ were distributed according to a normal distribution, setting λ=1 would imply a 68% confidence, λ=2 would represent 95% and λ=3 would represent a 99% confidence. For this system however, the statistics are more closely represented by a chi-square distribution so these confidence intervals are just approximations. A target is deemed benign, to a confidence determined by the value of λ, if $f_-\left(\lambda\right) > f_0$ for all templates, where f_0 is a specified cut-off value. Alternatively, the target is deemed dangerous if $f_+\left(\lambda\right) < f_0$. The test is inconclusive for targets for which neither test is true. There is flexibility in the system by adjusting the f_0 and the λ values. Setting a higher value of λ will result in fewer false-negatives but more false-positives. A lower value of λ will result in fewer false-positives but more false-negatives

For each experiment reported here, a single template was used and so L =1 and the subscript ℓ is not needed. The template responses were the averages of the explosive surrogate

net peak areas for each signature. Thus, the *i*th signature for a sample is N_i, given by Eq. (3), and the *i*th signature for the template is given by

$$\bar{N}_{ei} = \frac{1}{n}\sum_{j=1}^{n}\left(N_{ej}\right)_i \quad , \tag{8}$$

where $\left(N_{ej}\right)_i$ is the net peak area for the *j*th explosive surrogate for signature *i* and *n* is the number of explosive surrogate samples tested. Further, all samples were counted for the same length of time and thus $\beta = 1$. Thus, Eqs (5) and (6) take the simplified forms

$$\zeta = \sum_{i=1}^{N} \alpha_i \frac{\left(N_i - \bar{N}_{ei}\right)^2}{\sigma^2\left(N_i\right) + \sigma^2\left(\bar{N}_{ei}\right)}, \tag{9}$$

and

$$\sigma(\zeta) = 2\left[\sum_{i=1}^{N} \alpha_i^2 \frac{\left(N_i - \bar{N}_{ei}\right)^2}{\sigma^2\left(N_i\right) + \sigma^2\left(\bar{N}_{ei}\right)}\right]^{1/2}, \tag{10}$$

5.3 Results

Many different experiments were run throughout the course of this project. Initially, 10 gallon samples were used in a 1 m^3 aluminum box to simulate a car trunk. As the project progressed, the method was refined and smaller samples were used. Ultimately, 1 gallon containers inside a suitcase were decided upon to be the final testing arrangement. Experiments were done for both neutron and photon interrogation in the same configuration so the results could be combined. Two sets of experiments were conducted using the reactor in this final configuration. For each experiment, the region of interest function of Genie software was used to solve for the net area of each peak (N_i) and the error in that measurement, $\sigma(N_i)$. After the data were collected, the task of optimizing the results was next. The goal of using non-uniform weighting factors was to maximize the difference between the largest f_+ metric for the explosive surrogates and the smallest f_- metric for the inert materials. The weighting factors were chosen to optimize the results for both sets of experiments and are shown in Table 5.3 and were used in all FOM calculations.

Table 5.3. Weighting factors.

Element	Energy MeV	Weighting Factors
Oxygen	0.871	0.3
Carbon	1.262	0.2
Hydrogen	2.223	0.5
Nitrogen	2.31	0
Nitrogen	10.829	0

5.4 Nine Sample Experiment

For this experiment, four inert samples were used - polyethylene, rubber mulch, sand, and water. The explosive surrogates were FertA, FertB, and FertAB. FertAB was run at the beginning, end, and middle of the experiment for repeatability assessment. A numerical subscript was used to distinguish the multiple counts on FertAB. Each sample was placed in the suitcase and a 30 minute live time count was collected with the reactor at 500 kW. For this experiment, the average of the explosive surrogate responses and their errors, at each response energy, were taken to get the explosive template ($\bar{N}_{ei}$), and its standard deviation $\sigma(\bar{N}_{ei})$. The net counts for each sample, at each energy (N_i), can be seen in Table 5.4, and the standard deviations are given in Table 5.5. For each sample, equations (7), (9) and (10) were applied to get the results shown in Table 5.6.

Table 5.4. Net area for each signature in nine sample experiment.

Sample	0.871 MeV	1.262 MeV	2.223 MeV	2.31 MeV	10.829 MeV
FertA	12920	1080	24731	464	9
FertB	12336	877	23532	298	4
FertAB1	11617	955	22561	287	5
FertAB2	11832	877	23223	0	7
FertAB3	12401	1185	23961	0	11
Polyethylene	12371	919	26881	0	2
Rubber	12319	703	23486	331	9
Sand	11300	920	20566	326	2
Water	11838	849	25734	0	12
Explosive Template	12221	995	23602	210	7

Table 5.5. Standard deviations for each signature in the nine sample experiment.

Sample	0.871 MeV	1.262 MeV	2.223 MeV	2.31 MeV	10.829 MeV
FertA	181	114	183	24	3
FertB	183	119	184	19	2
FertAB1	177	104	179	17	2
FertAB2	181	133	181	0	3
FertAB3	196	132	182	0	5
Polyethylene	199	124	190	0	1
Rubber	184	112	186	22	3
Sand	172	110	177	18	1
Water	195	111	190	0	4
Explosive Template	184	120	182	12	3

Table 5.6. Results from nine sample experiment.

Sample	ζ	$\sigma(\zeta)$	$f_{-}(\lambda=1)=\zeta-\sigma(\xi)$
Polyethylene	77.89	12.98	64.91
Rubber	0.77	1.38	-0.61
Sand	75.63	14.34	61.29
Water	33.65	9.32	24.33
Explosive surrogate	ζ	$\sigma(\zeta)$	$f_{+}(\lambda=1)=\zeta+\sigma(\xi)$
FertA	11.84	6.21	18.05
FertB	0.19	0.81	1.01
FertAB1	10.01	5.60	15.61
$FertAB_2$	1.86	2.64	4.50
$FertAB_3$	1.34	2.22	3.56

As false-negatives are considered more important than false-positives, a f_o value of 20 could be chosen to distinguish between inert and explosive material. This f_o results in zero false-negatives and one false-positive for rubber. These results are reasonable, but not ideal. The confidence interval is only $\lambda=1$, and to decrease the f_o to have zero false-positives would result in five false-negatives. The repeatability of the experiment can also be improved upon. The figure of merit for FertAB varied from 3.56 to 15.61. This is less than a 2σ variation but it would be good if $\sigma(\zeta)$ could be reduced.

5.5 Fourteen Sample Experiment

The next experiment was conducted with the goal of testing more samples, and collecting data for a longer time to get better results. Each sample was irradiated at 500 kW and a 45 minute live time count was done with the experiment spread out over three days. Aluminum, chalk, polyethylene, rubber mulch, sand, water, and an empty can were used for inert samples. For the explosive surrogates, FertA, FertB and ammonium nitrate were used and FertAB was run four times for repeatability. Again, the average of the explosive surrogate responses and their errors, at each response energy, were taken to get the explosive template ($\bar{N}_{ei}$), and its variance $\sigma^2(\bar{N}_{ei})$. The net counts for each sample, at each energy (N_i), can be seen in Table 5.7, and the standard deviation for each area, $\sigma(N_i)$, is given in Table 5.8. For each sample, equations (7), (9), and (10) were applied to get the results shown in Table 5.9.

Table 5.7. Net area for each signature in fourteen sample experiment

Sample	0.871 MeV	1.262 MeV	2.223 MeV	2.31 MeV	10.829 MeV
FertA	17610	1345	36923	703	16
FertB	17620	1235	37471	451	15
FertAB1	17485	1487	37561	435	17
FertAB2	18355	1771	38317	343	12
FertAB3	16542	1526	35753	297	18
Polyethylene	18301	1538	43185	396	15
Rubber	18534	1370	39965	501	11
Sand	16707	1251	34134	494	11
Water	16015	1483	39876	0	14
Aluminum	17477	1297	35006	0	10
Ammonium Nitrate	17654	1660	39274	674	17
Chalk	15421	1513	32894	0	6
Empty	15636	1314	33461	554	1
FertAB4	16543	1402	36368	631	15
Explosive Template	17401	1489	37381	505	16

Table 5.8. Variance for each signature in fourteen sample experiment.

Sample	0.871 MeV	1.262 MeV	2.223 MeV	2.31 MeV	10.829 MeV
FertA	223	135	225	27	5
FertB	213	140	229	23	4
FertAB1	222	138	225	18	5
FertAB2	246	138	230	19	3
FertAB3	203	133	221	17	6
Polyethylene	227	143	242	21	4
Rubber	224	126	236	22	3
Sand	208	132	215	24	3
Water	205	135	235	0	5
Aluminum	213	136	217	0	5
Ammonium Nitrate	208	165	236	27	4
Chalk	196	135	220	0	2
Empty	219	133	221	23	1
FertAB4	215	149	233	24	6
Explosive Template	219	143	228	24	5

Table 5.9. Results from fourteen sample experiment.

Sample	ζ	$\sigma(\zeta)$	$f_{-}(\lambda=1)=\zeta-\sigma(\xi)$
Aluminum	28.62	8.08	20.54
Chalk	113.74	18.24	95.49
Polyethylene	154.55	19.25	135.30
Rubber	34.96	10.29	24.67
Sand	55.46	12.22	43.24
Water	35.40	10.40	25.00
Air (empty can)	85.98	16.12	69.87
Sample	ζ	$\sigma(\zeta)$	$f_{+}(\lambda=1)=\zeta+\sigma(\xi)$
FertA	1.26	2.12	3.39
FertB	0.52	1.22	1.73
$FertAB_1$	0.18	0.73	0.91
$FertAB_2$	7.09	5.19	12.29
$FertAB_3$	15.61	6.93	22.54
$FertAB_4$	7.21	4.95	12.16
Ammonium nitrate	16.94	6.58	23.52

These results were better but could still be improved upon. Again, only a λ=1 confidence value could be used. Here, if a f_o value of 24 was used, there would be no false-negatives, no

false-positives, and one inconclusive for aluminum. The repeatability was improved from the last experiment with the longer count time. In this case, the f_i filter function values for FertAB varied from 0.91 to 22.54. Considering a total range of 135, this may be considered acceptable.

The repeatability variations were likely the result of a number of factors. The largest contributor was most likely power fluctuation in the reactor. As previously stated, the reactor was brought up to 500 kW and held there for the entirety of the experiments. This power level was determined to be the highest the reactor could sustain for the several hours the experiments took place. As the heat effects within the reactor decreased reactivity, the control rods had to be withdrawn to maintain power. This was done several times throughout the experiment resulting in jumps and gradual drops in power level. A 1% change in reactor power could have represented a several hundred count difference in some cases. Repeatability variations could have also been the result of the way the peak areas were solved for using the ROI function. There was a certain degree of judgment as to where the peaks started as it was visually selected by the operator. This may not have been identically selected for each peak resulting in variation in peak areas.

CHAPTER 6 - Summary and Recommendations

The research into SBRS suggests it is possible to differentiate dangerous targets that may contain as little as 3.8 L (1 gal or about 7 kg) of explosive material from targets whose contents are benign. While the results were not perfect, the analysis did show that this could be achieved with no false-negatives and minimal false-positives with approximately 68% confidence.

The greatest advantage of SBRS is that the entire technique can be automated and human interpretation can be removed. Once signatures are collected, they are automatically compared to explosive library template responses. The system will then simply display to the operator a green light for an inert sample, a red light for a potentially dangerous sample, or a yellow light if the test is inconclusive. The SBRS system will require minimal user interface and training to operate.

Neutron-based methods also have the ability to scan denser materials than other explosive detection methods. This method has highly penetrating radiation for both the incident and generated radiation. Neutrons in general, and especially high energy neutrons, will be able to penetrate deep into a target. The generated prompt gamma rays and inelastically scattered gamma rays have high energies, and are more likely to escape the target and reach the detector.

SBRS also has the potential to be a true stand-off technology. All radiation-based methods suffer from signal fall off as a function of distance. With this method, a slowly diverging beam of neutrons can be produced using a collimator but then the scattered and generated radiation fluxes will vary as $1/r^2$, where r is distance from the target. However, with the highly penetrating nature of both the incident and generated radiation, this method has the potential to operate at distances up to several meters.

The SBRS method is also highly adaptive. Different responses, as well as the different values of f_o, weight factors, and λ can be used depending on conditions and specific threats. Additional signatures can be added to the system analysis such as the weight of the target. The SBRS method also has the potential to be used for more than just explosive detection. This method could be adapted to look for contraband material such as drugs.

The challenge with SBRS will be creating a large enough template library to be able to identify the explosives. Templates have to be created for different sizes and shapes of

explosives, in different configurations with respect to the detector and source. Then, variations of each of these templates will need to be constructed for various "clutter" scenarios of having miscellaneous material packed around them. However, once a sufficient library is created, the system will only improve with use as more templates are added and the library of templates is tailored to current threats.

6.1 Future Work

One of the difficulties in differentiation of the targets was the few viable signatures that were generated. In the end, none of the inelastically scattered gamma rays were useful because so few counts were collected. The inelastic scatter gamma responses had large uncertainty and did not differentiate well among the samples. The 10.829 MeV would also be a good indication of nitrogen, but again, the low number of those capture gamma rays collected resulted in high uncertainty and poor distinction among samples.

To help improve the differentiation, a deuterium on tritium target (D-T) neutron generator is in the process of being ordered. The D-T generator will improve results in two ways. The average neutron energy of a D-T generator is around 14 MeV, which will allow for the excitation of many more inelastic scatter gamma rays. The intensity of the collimated beam from the D-T generator, with a source strength of around 10^{11} n cm^{-2} s^{-1}, will be substantially higher than the intensities of the beams from the tangential beam tube or the Cf-252 source. This will allow for shorter signature collections times.

A new gamma-ray detector is also being ordered which will be electrically cooled. The current HPGe detector is 20% efficient, and has to be cooled by liquid nitrogen, which presents a serious problem for a field prototype. The new detector is 80% efficient, which will further reduce count times.

Ultimately, the results from these preliminary experiments have shown that SBRS has the potential to identify small amounts of explosives at several meters distance, quickly, and with high sensitivity and good specificity.

References

[1] *Iraq Coalition Causality Count.* June 2008. Deaths Caused by IED. 1 July 2008 <http://icasualties.org>.

[2] Chisholm, P. (Sep 12, 2005). Clearing the Roads. *Special Operations Technology Online Archives*, Volume 3 Issue 6.

[3] Wilson, C. (February, 2006). Improvised Explosive Devices (IEDs) in Iraq: Effects and Countermeasures. *Congressional Research Service Report for Congress*.

[4] Global Security (2007). *Improvise Explosive Devices (IEDs) / Booby Traps*. Retrived July 7, 2008 from, http://www.globalsecurity.org/military/intro/ied.htm

[5] Guzman, R. (2007) ARNEWS. *Joint IED Task Force Helping Defuse Insurgency's Threat*. Retrieved July 7, 2008. http://www4.army.mil/ocpa/read.php?story_id_key=7618

[6] Singh, S. Singh, M. "Explosives Detection Systems (EDS) for Aviation Security." Signal Processing 83 (2003) : 31-55

[7] Annis, M. Bjorkholm, P. Schafer, D. Atomic detection of explosives using X-ray imaging, in: T.P. Tsccounmis (Ed.), Access Security Screening Challenges and Solutions, ASTM STP 1127, American Society for Testing and Materials, Philadelphia, 1992, pp. 68-81

[8] Pettersson, A. Wallin, S. Brandner, B. Eldsater, C. Holmgren, E. "Explosives Detection – A technology Inventory." FOI 2030 (2006) : ISSN 1650-1942

[9] Harding, G. Gilboy, W. Ulmer, B. "Photon-induced positron annihilation radiation (PIPAR) – A novel gamma ray imaging technique for radiographically dense materials" Nuclear Instruments & Methods In Physics Research 398 (1997) : 409-422

[10] Gozani T. "The role of neutron basd inspection techniques in the post 9/11/01 era" Nuclear Instruments & Methods 213 (2004) : 460-463

[11] Hannum, D. Parmeter, J. "Survey of Commercially Available Explosives Detection Technologies and Equipment" Sandia National Laboratories September 1998

[12] "The Honey Trap." Engineering and Technology December 2007: 24-26

[13] Molnar, Gabor, ed. Handbook of Prompt Gamma Activation Analysis. Dordrecht, The Netherlands: Kluwer Academic Publishers, 2004

[14] Buffler, A. "Contraband Detection Using Neutrons" University of Cape Town. Department of Physics http://www.phy.uct.ac.za/people/buffler/FNSA.pdf

[15] M. Kasaishi, A. Tojo, M. Furuta, H. Takayama, I. Miyazaki, T. Shimizu, M. Shibata, K. Kawade, A. Taniguchi. "Calculations of an HPGe Detector Peak Efficiency Curve up to 11 MeV with EGS4 and GEANT4" NDS Proceedings (2004)

[16] Nuclear Power Fundamentals. Nuclear Physics and Reactor Theory Volume 1 of 2 < http://www.tpub.com/content/doe/h1019v1/css/h1019v1_137.htm>

[17] C. Sublette "Nuclear Weapons Frequently Asked Questions" Nuclear Weapon Archive July 2008 < http://nuclearweaponarchive.org/Library/Fission.html>

[18] R.C. Martin, J.B. Knauer, P.A. Balo. "Production, Distribution, and Applications of Californium-252 Neutron Sources" IRRMA '99

[19] Dunn, W.L., R. Brewer, K. Loschke, and J. Lowrey (2007), Radiation Interrogation Using Signature Analysis for Detection of Chemical Explosives, Proc. IEEE Conference on Technologies for Homeland Security: Enhancing Critical Infrastructure Dependability, Boston, MA, 16-17 May, 2007, pp. 7-12.

[20] Gabor L. Molnar. Handbook of Prompt Gamma Activation Analysis. Dordrecht: Kluwer Academic Publishers, 2004.

[21] Canberra Inc. "Standard Electrode Coaxial Ge Detectors" Canberra Products. September 7, 2008 < http://www.canberra.com/products/486.asp>

[22] Shultis, Kenneth, and Richard Faw. Radiation Shielding. Upper Saddle River: Prentice Hall PTR, c1996

Appendix A - Sample MCNP5 Input Dataset

```
A shield box around a point Cf-252 source
c
c
c   VIEW TOWARD      +----------------------+
c   ENTRANCE         | +------------------+ |
c   SLOT             | |       ^ x-axis  | |
c                    | |       |         | |
c   (z-axis into     | |       |         | |
c    the plane       | |    +-----+      | |
c                    | |    |--o--|------| |-----> y-axis
c                    | |    +-----+      | |
c                    | |                 | |
c                    | |                 | |
c                    | |                 | |
c                    | +------------------+ |
c                    +----------------------+
c
c
c ************** BLOCK 1 -- CELL CARDS **********************
c  unit's outer housing
 100  3 -1.00   126 -111 112 -115 113 -114
             (121:-122:-123:124:125:-126)
             imp:n=1          $ housing less duct wall
 101  3 -1.00   116 -126 112 -114 113 -111
             (21:-22:-23:24:126:-116)
             imp:n=1          $ housing wall w duct entrance
c  innards
 103  0        -121 122 123 -124 -125 126    imp:n=1 $ void inside unit
```

```
 104  0        -21 23 22 -24 -126 116        imp:n=1 $ entrance void
c beam duct
 1  3  -1.00   -11 12 13 -14 -116 200
           (21:-23:-22:24:116:-200)   imp:n=1  $ duct housing
 3  0        -21 23 22 -24 -116 200     imp:n=1  $ duct void
c cells outside -- graveyard
 4  0   -116 (-200:11:-12:-13:14)    imp:n=0  $ void outside left
 5  0    116 (111:-112:-113:114:115) imp:n=0  $ void outside right

c ************** BLOCK 2 -- SURFACE CARDS ******************
c SHIELD HOUSING SURFACES
c   outsurfaces (4" thick walls)
 111 PX   25.40   $ top outer  wall (10")
 112 PY  -25.40   $ back outer wall (10")
 113 PX  -25.40   $ bottom outer wall (-10")
 114 PY   25.40   $ front outer wall (10")
 115 PZ   25.40   $ right outer wall (10")
 116 PZ  -25.40   $ left outer wall (10")
c  inside walls of unit  (1' x 1' x 1')
 121 PX   15.24   $ top outer  wall (6")
 122 PY  -15.24   $ back outer wall (6")
 123 PX  -15.24   $ bottom outer wall (-6")
 124 PY   15.24   $ front outer wall (6")
 125 PZ   15.24   $ right outer wall (6")
 126 PZ  -15.24   $ left outer wall (6")
c
c  DUCT SURFACES
c  outer duct walls (walls 4"thick)
 11 PX  12.70   $ top outer duct wall (5")
 12 PY  -12.70  $ back outer duct wall (5")
 13 PX  -12.70  $ bottom outer duct wall (-5")
```

```
 14 PY  12.70   $ front outer duct wall (5")
c   Inside duct walls (2" x 2")
 21 PX  2.54    $ top inner duct wall (1")
 22 PY  -2.54   $ back inner duct wall (-1")
 23 PX  -2.54   $ bottom inner duct wall (-1")
 24 PY  2.54    $ front inner duct wall (1")
c   vertical plane for end of duct (duct walls 12" long)
 200 PZ -55.88  $ duct mouth (1' from outer shld surface)

c ************** BLOCK 3 -- COMMAND CARDS ******************
mode n             $ track neutrons
nps  300000000       $ no. of fission neutrons to track
c  void
c
c  Point fission Cf-252 source
SDEF POS 0 0 0  ERG=d1  PART=1
SP1  -3  1.025  2.926   $ Watt spectrum for Cf-252
c  PRINT 110     $-- print data for first 50  starting electrons
c
c
C  Tally 2: dose averaged over the entrance to the irradiator
F2:n  116  115 200          $-- use flux detector at duct entrance
FS2  21 -22 -23 24          $-- segments of surface 116
c  --areas of scoring segments
SD2  1161.288  638.708  638.708  116.128  25.8064
     1161.288  638.708  638.708  116.128  25.8064
      258.064  154.834  154.834  51.613   25.8064
c  ------------------------------------------------------------
c   Modify tally to give dose rate for Cf-252 source:
c   mrem/h = rem/neut x neuts/s x 1000 mrem/rem x 3600 s/h
c   For KSU's Cf-252 (on 21/09/06 will get 4.11E7 neuts/sec
```

```
c   THUS  mrem/h = (rem/neut) x 4.11E7 x 1000 x 3600
c         mrem/h = (rem/neut) x 1.48E14
c  ------------------------------------------------------------
FM2  1.48E14
FC2  Dose is in mrem/h for CF-252 source on 21/09/06
c ------------------------------------------------------------------
c  ambient neutron dose equiv. H*(10mm) [rem cm^2] (from T-D3 of S&F)
c  Plane parallel (PAR) neutrons incident on ICRP sphere.
c ------------------------------------------------------------------
de2    2.500E-08 1.000E-07 1.000E-06 1.000E-05 1.000E-04 1.000E-03
       1.000E-02 2.000E-02 5.000E-02 1.000E-01 2.000E-01 5.000E-01
       1.000E+00 1.500E+00 2.000E+00 3.000E+00 4.000E+00 5.000E+00
       6.000E+00 7.000E+00 8.000E+00 1.000E+01 1.400E+01 1.700E+01
       2.000E+01
df2    8.000E-10 1.040E-09 1.120E-09 9.200E-10 7.100E-10 6.200E-10
       8.600E-10 1.460E-09 3.500E-09 6.900E-09 1.260E-08 2.580E-08
       3.400E-08 3.620E-08 3.520E-08 3.800E-08 4.090E-08 3.780E-08
       3.830E-08 4.030E-08 4.170E-08 4.460E-08 5.200E-08 6.100E-08
       6.500E-08
c
c  Tally 12: MCA spectrum with bins of width .01 MeV over (0,5.0)MeV
F12:n  116 200           $-- flux at entrance & exit of duct
FS12  21 -22 -23 24          $-- segments of surface 116 & 200
c  --areas of scoring segments
SD12  1161.288  638.708  638.708  116.128  25.8064
     258.064   154.834  154.834  51.613   25.8064
E12 0.0 99I 10.0             $-- set up energy channel grid
c
c  Write output source file: photons only leaving the irradiator
c  SSW -116(2 3) PTY n
c
```

```
c
c                    MATERIALS
c ---------------------------------------------------------------------
c      material: borated polyethylene d=1.00 g/cm^3  CH2 + 8 wt% B4C
c              B-11 5.029; B-10 1.234; C 80.595; H 13.143
c ---------------------------------------------------------------------
m3    1001.50c -0.13143
      5010.50c -0.01234
      5011.50c -0.05029
      6000.50c -0.80594
MT3  poly.60t
```